University of Bremen, Department of Marine Zoology
Fachbereich 2 Biologie/Chemie

Metabolism and Physiological Adaptations of Pelagic Copepods in the Northern Benguela Current Ecosystem

Master Thesis

As a pre-requisite of the

MSc. Programme in Marine Biology

by

Maya Bode

Bremen, July 2011

1. Examiner:

PD Dr. Holger Auel

Dept. of Marine Zoology

University of Bremen

2. Examiner:

Dr. Werner Ekau

Dept. of Ecology
WG Fisheries Biology

Leibniz Center for Tropical Marine Ecology

Contents

List of Abbreviations

ATP	**Adenosine triphosphate**
C5	**Copepodite stage C5**
C2/3	**Copepodite stage C2 or C3**
DVM	**Diel vertical migration**
ETS	**Electron transport system**
GENUS	**Geochemistry and Ecology of the Namibian Upwelling System**
INT	**2-(p-jodophenyl)-3-(p-nitrophenyl)-5-phenyl tetrazolium chloride**
IOML	**Intermediate oxygen minimum layer**
LDH	**Lactate dehydrogenase**
LME	**Large marine ecosystem**
NADH	**Nicotinamide adenine dinucleotide**
NADPH	**Nicotinamide adenine dinucleotide phosphate**
IOML	**Intermediate oxygen minimum layer**
RV	**Research vessel**
SST	**Sea surface temperature**

List of Figures

List of Tables

Abstract

Copepods are the most abundant components of mesozooplankton communities throughout the world's ocean. They play a key role in the marine ecosystem as a linkage between primary producers and higher trophic levels as well as within the biological carbon pump by enhancing the vertical flux of organic matter from the euphotic zone to the deeper layers. Metabolic rates give an estimate of the copepods' production and energy expenditure which helps to understand nutrient and carbon fluxes in the marine ecosystem. This study was focused on the aerobic and anaerobic metabolism of different copepod species from the northern Benguela Current system. Copepod samples were collected from different depth layers between Walvis Bay and Lüderitz off the Namibian coast in February 2011.

Individual respiration rates varied from 0.003 to 0.061 µmol O_2 h^{-1} Ind^{-1}, while mass-specific rates were in the range of 17 to 157 µmol O_2 h^{-1} g DM^{-1}. The respiration rates were positively correlated with activities of the respiratory electron transport system (ETS) whereas the ETS-activities ranged from 0.006 to 0.199 µmol O_2 h^{-1} Ind^{-1} and 14 to 125 µmol O_2 h^{-1} g WM^{-1}. The ratios of respiration to ETS-activities varied between 0.1 and 0.6. Surface *R. nasutus* and deeper-living *E. hyalinus* exploited merely 10 and 16% of their potential metabolic rates for respiration. Diapausing copepodids C5 of *Calanoides carinatus* had severely reduced ETS-activities. Temperature had a significantly positive effect on copepods' respiration. Q_{10} values varied from 2 to 6.8 while *Eucalanus hyalinus* and *Rhincalanus nasutus* showed the highest Q_{10}, *Pleuromamma quadrungulata* the lowest. Both individual respiration rates and ETS-activities increased while mass-specific rates and activities decreased with increasing body mass. Using the allometric function of $R = a W^b$, the scaling coefficient b was 0.728 and 0.541 for individual respiration rates and ETS-activities, respectively. In contrast, the scaling coefficient for mass-specific respiration rates and ETS-activities was – 0.272 and – 0.459. Lactate dehydrogenase (LDH) activities in the different species ranged from 2.3 to 39.5 U g WM^{-1} while *R. nasutus* had by far the highest activities. In contrast to the aerobic metabolic rates, mass-specific LDH-activities increased significantly with increasing body mass.

By means of the R:ETS ratio, respiration rates may be estimated from ETS-activities, although the ratios seemed to be species- and depth-related. The high Q_{10} values of the Eucalanidae suggest that these species, that do not undergo diel vertical migrations and have a rather lethargic lifestyle, are not adapted to rapid temperature changes. In contrast, *P. quadrungulata*, an extensive vertical migrator, tolerated wide temperature changes. The low metabolic rates and high LDH-activities in *R. nasutus* suggest an adaptation to oceanic intermediate oxygen minimum layers. Not only body mass and temperature, but also environmental factors such as oxygen and depth as well as behaviour and activity levels appeared to influence the copepods' metabolism. Applying multiple regression analysis with body mass and temperature as parameters, first steps were made to model copepods' consumption and energy requirements within the Benguela Current ecosystem.

1. Introduction

Large marine ecosystems (LME), as the Benguela Current, are unique concerning their bathymetry, hydrography, productivity and trophic relationships. 90% of the global production of fish and other marine resources originates within these LMEs (Sherman 2006). Besides the California, Humboldt and Canary Currents, the Benguela Current belongs to the four major eastern boundary currents and coastal upwelling systems of the World's Ocean. Together with the Humboldt Current, the Benguela system is the most productive upwelling system reaching an average annual primary production of 1.25 kg C m^{-2} yr^{-1} (Boyer and Hampton 2001, Shannon and O'Toole 2003). Despite of high primary production, the biomass of economically important fish, such as anchovy, sardine, herring and hake, has been decreasing since the 1970s not only due to overfishing but also because of environmental changes during the last decades (Boyer and Hampton 2001, Heymans et al. 2004). This study is part of the GENUS project (Geochemistry and Ecology of the Namibian Upwelling System) which is aimed to resolve and model the relationships between climate change, biogeochemical cycles of nutrients, climate relevant gases and ecosystem structures within the Benguela upwelling system. The short food chains, characteristic for upwelling regions, are ideal to quantify trophic interactions and energy flows within the ecosystem (Sommer et al. 2002).

As dominant primary consumers, zooplankton displays an important linkage of primary production with production of organisms at higher trophic levels (Longhurst 1985, Ikeda et al. 2007). Copepods are the most abundant components of mesozooplankton communities in all marine regions. Total contribution of copepod biomass to the mesozooplankton was estimated to be 44 – 55% in the tropical western Pacific Ocean (Heinrich 1969), 67 – 70% in sub-Antarctic and Antarctic waters (Hopkins 1971), 80% in the Sargasso Sea (Verity 1985) and 83 – 89% in Arctic waters (Hopkins 1969). Moreover, pelagic copepods play an essential role within the biological carbon pump (Longhurst and Harrison 1989). Many species undergo diel and ontogenetic vertical migrations (DVM, OVM). The most common form of DVM is the nocturnal migration: copepods feed in the upper surface layers at night and migrate into deeper layers when light intensities increase, presumably to avoid predation (Mauchline 1998). At depth, the animals respire, produce faecal pellets or may

be eaten by deeper-living carnivores enhancing the vertical flux of organic matter from the euphotic zone to deeper layers (Mauchline 1998, Wilson and Steinberg 2010). The annual copepod production for the Angola-Benguela frontal region and the southern Benguela upwelling system was estimated to be 39 g C m^{-2} yr^{-1} and 99 g C m^{-2} yr^{-1}, respectively (Richardson et al. 2001, Verheye et al. 2005). Comparatively few data exist for the northern Benguela ecosystem (Verheye et al. 2005).

Upwelling regions are highly variable ecosystems, e.g. concerning food availability, dissolved oxygen and water temperature. Thus, species living in these systems need to be well adapted in terms of reproduction, growth and population maintenance (Jarre-Teichmann et al. 1998, Peterson 1998). Within the northern Benguela sub-system off the Namibian coast, zooplankton communities are dominated perennially by the calanoid copepod *Calanoides carinatus* (Verheye et al. 1991, 1992). Furthermore, *Metridia lucens, Centropages brachiatus*, *Nannocalanus minor*, *Aetideopsis carinata, Pleuromamma spp., Eucalanus hyalinus and Rhincalanus nasutus* are abundant (Timonin 1997, Peterson 1998, Loick *et al*. 2005, Auel and Verheye 2007). The key species *C. carinatus* exhibits a highly adaptive life cycle characterized by OVMs (Kosobokova et al. 1988, Verheye 1991, Verheye et al 1991, Timonin et al. 1992, Verheye and Field 1992, Arashkevich et al. 1996, Auel et al. 2005, Verheye et al. 2005). Reproduction takes place on the shelf within the upwelling region. A part of the population is transported to the open ocean by Ekman-drift and descends as copepodite stages C5 to about 400 to 800 m depth where they overcome periods of food shortage in a dormant stage. Eventually they are brought back to the shelf by new upwelling events to ensure their population's maintenance within the coastal upwelling system (Verheye et al. 1991).

Due to their essential role in the cycling of organic matter in the ocean, understanding the copepods' metabolism is of vital importance to estimate their contribution to oceanic biogeochemical cycles of carbon and other elements within the marine ecosystem. Physiological processes as ingestion and growth in zooplankton are difficult to assess because the knowledge about their natural food is limited and require more time for incubation and experimentation (Ikeda 1985). In contrast, measurements of metabolism are much more practicable. Respiration measurements provide information of the minimal food, thus, energetic requirements of an animal and are good estimates of its metabolic

rates (Ikeda 1985, Ikeda et al. 2000). Within the GENUS project it was agreed to measure *in situ* respiration rates for as many copepod species as possible.

The direct determination of respiration rates involves the incubation of copepods in a controlled system. These methods are still time-consuming and imply sampling and capture stress to the animals (Owens and King 1975, Schalk 1988). The respiratory electron transport system (ETS) assay was introduced as a biochemical measure of the potential metabolic rate to estimate the potential plankton respiration (Packard 1971). This method was supposed to circumvent problems of time, stress, starvation, crowding and bacterial growth (Hernandez-Léon and Gómez 1996).

The distribution and abundance of copepods is dependent on water masses and abiotic factors whereas temperature and oxygen are central parameters. Climate induced changes as increased temperatures or expansion of hypoxic zones within the pelagic zone are expected to affect the marine ecosystem structure and its food webs in future (Ekau et al. 2010). To understand and model possible consequences of climate change, a better understanding of physiological tolerances, adaptations and constraints of key species within a certain ecosystem is necessary. Species from highly variable ecosystems as upwelling regions are ideal to study the impact of changing environmental factors on their physiology. The positive effect of temperature on biochemical reaction rates is described as the Q_{10} value (Somero and Childress 2002). For metabolic processes in copepods a Q_{10} value between two and four was derived, whereas the value varies with the physiology and behavioural pattern of the animals (Mauchline 1998).

Intermediate oxygen minimum layers (IOML) are associated with the Humboldt and Benguela upwelling systems, the Arabian Sea and the Bay of Bengal (Helly and Levin 2004). They are characterized by low temperatures and continuously low oxygen concentrations of less than 1.4 ml O_2 L^{-1} at depths between 60 and 500 m (Verheye and Ekau 2005, Auel and Verheye 2007, Ekau et al. 2010). IOMLs influence the vertical distribution and migratory patterns of copepods by acting as a barrier. Non-tolerant species are restricted to the thin surface layer or the layers below the IOML while biomass of mesozooplankton within the IOML is severely reduced (Wishner et al. 2000). Low oxygen levels may cause changes in different organizational levels, e.g. from individual life cycle performances, growth rates and reproduction to changes in trophic relationships and regime shifts in

certain ecosystems (Ekau et al. 2010). Some organisms living in or passing through the IOML are expected to be adapted to some extent in their energy metabolism to the hypoxic environment as oxygen tolerance varies with different species. For instance, fish larvae may already be affected at oxygen concentrations less than 3 ml O_2 L^{-1}, whereas euphausiids may survive down to 0.1 ml O_2 L^{-1} (Ekau et al. 2010).

Other ecological and physiological factors have been identified to influence the metabolic rate, e.g. body mass (Ikeda 1970, 1974, 1985, Ikeda et al. 2001, Ivelva 1980), pressure (Childress 1977), regional and seasonal variability (Conover 1959), activity (Pfaffenhöfer 2006), feeding behaviour (Conover 1960), and DVMs (Pavlova 1984). Allometric models may be applied to assess ecological flows in certain ecosystems because organism size may be applied as a basis for characterizing marine plankton communities (Moloney and Field 1989). Since body mass and temperature have been identified as the most important influencing factors, their combined effect on respiration in zooplankton may be used to establish generalized features of metabolic rates (Ikeda 1985, Ikeda et al. 2001).

In general, physiological and biochemical aspects of copepods have been little studied. The five main objectives of this study were 1) to analyze the respiration rates and ETS-activities of different copepod species from the northern Benguela Current upwelling system, 2) to improve the ETS-assay and give a recommendation concerning its valuation in replacing respiration measurements, 3) to estimate the dependence of respiration rates on temperature and other ecological and physiological factors, 4) to measure LDH-activities of different species and estimate the copepods' anaerobic metabolism, and 5) to develop a mathematical model to predict respiration rates from the copepods' body mass and habitat temperature.

Respiration measurements on different copepod species were performed at simulated *in situ* and manipulated temperatures (*in situ* temperature ± 5°C). For the same species ETS-activities were measured. By comparing the *in vivo* respiration rates and ETS-activities, it was calculated how much the animal exploits of its potential metabolism for respiration. The ETS-assay is critically discussed whether it is a useful method to estimate the copepods' *in vivo* respiration rates, which would simplify and accelerate future respiration studies. Q_{10} values for the different species were calculated and possible environmental, physiological and behavioural factors are discussed that may influence the metabolic rates

of the animals. Furthermore, LDH-activities of different copepod species were measured to assess the contribution of anaerobic pathways to possible physiological adaptations to oceanic IOML. Combining the effect of body mass and temperature, a mathematical model was developed to predict the metabolic rates of copepods from these parameters.

Hypothesis 1:

The ETS-activity is positively correlated with the measured respiration rates of the copepods.

While respiration rates rather estimate the routine metabolism, the ETS-assay detects the potential metabolic rate of the organism. Thus, it is expected to exceed the respiration rate by far.

Hypothesis 2:

Copepod species that conduct diel vertical migrations have lower Q_{10} values than species resident in a certain depth layer.

Migrating copepods experience substantial temperature changes of more than 10°C on their nightly ascent to the surface. Hence, these species are expected to be adapted to rapid temperature changes which may be expressed by a higher temperature tolerance, thus, lower Q_{10} values. Lower Q_{10} values would limit the sensitivity of their metabolic rates to changing temperatures.

Hypothesis 3:

Copepods that potentially live in the intermediate oxygen minimum layer show higher LDH-activities.

Anaerobic metabolism is a possible adaptation in animals occurring in IOMLs within the ocean to maintain their metabolic rates under unfavourable environmental conditions.

2. Materials and Methods

2.1. Study Area

The Benguela current system is situated along the West Coast of Africa in the South-East Atlantic Ocean. The north-flowing cold Benguela Current stretches from Cape of Good Hope (34°S) in South Africa equatorwards to the Angola Front at ca. 16°S (Shannon et al. 2006). A unique feature of the Benguela Current is its enclosure within two warm water regimes: In the north the tropical warm Angola Current flows southwards along the Angolan coast and meets the Benguela Current at the Angola-Benguela Frontal Zone, while in the south the Benguela Current mixes with the south-flowing Indian Ocean western boundary Agulhas Current and its retroflection area (Figure 1) (Shannon et al. 1987, Shannon and Nelson 1996). Waters of the Angola Current enter the Benguela system as a poleward undercurrent and bring low-oxygen water to the northern Benguela system below the seasonal thermocline creating a permanent intermediate oxygen minimum layer (IOML) with oxygen concentrations of less than 1 ml O_2 L^{-1} between 270 and 400 m depth (Lass et al. 2000, Duncombe Rae 2005).

The south-easterly trade winds along the southern African coast are modified by seasonal low pressure cells over the continent and eastward moving cyclones in the south (Nelson and Hutchings 1983). The upwelling centre at Lüderitz (~26°70'S 15°E) experiences upwelling throughout the year and divides the ecosystem into two sub-systems: the northern and the southern Benguela system. Upwelling-favourable, south-easterly trade winds are promoted during spring and summer in the southern and during autumn and spring in the northern Benguela region (Shannon and O'Toole 2003). Phytoplankton biomass reaches maximum chlorophyll a values in summer in the southern Benguela system and in winter in the northern. Persistent phytoplankton maxima may be observed on the central Namibian shelf and the South African west coast shelf. On the contrary, phytoplankton biomass is perennially low at Lüderitz, presumably caused by strong turbulent mixing (Hutchings et al. 2006). Zooplankton biomass is slightly increased off Walvis Bay in the second half of the year but no clear signal is evident that couples upwelling, phytoplankton and zooplankton abundance (Hutching et al. 2006). Sampling

was focused exclusively on the northern Benguela ecosystem extending from 23° to 26° 40’ S.

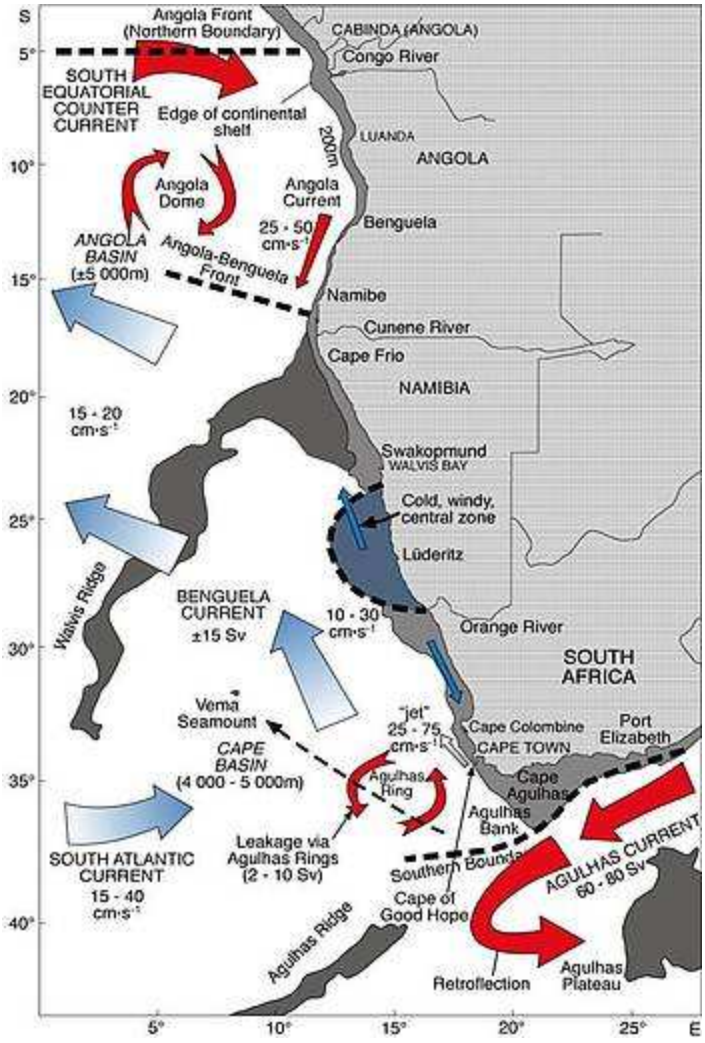

Figure 1: Bathymetric features, surface currents and boundaries of the Benguela upwelling system, red arrows indicate warm currents, blue cold (Shannon 2006).

2.2. Sampling

Samples and respiration data were collected during leg 1 of the GENUS (Geochemistry and Ecology of the Namibian Upwelling System) research cruise onboard the RV Maria S. Merian from January 30th until February 9th. Copepod samples were taken at twelve stations in the northern Benguela Upwelling System between Walvis Bay and Lüderitz (Figure 2).

Two cross-shelf transects at respectively 23°S and 26°40’ S and various stations in between were chosen for sampling (Figure 2). Copepod samples were taken from stratified hauls using different multiple opening/closing net systems: double and single Multiple Opening/Closing Net and Environmental Sensing System (MOCNESS, mesh sizes 333 µm and 1000 µm), vertical double oblique Multinet hauls with 55 to 500 µm mesh sizes (Hydrobios Multinet Midi). Copepod samples derived from six specific depth layers: 50 – 25 m, 75 – 50 m, 100 – 50 m, 400 – 200 m, 600 – 400 m, 800 – 600 m. Only animals in fit and healthy condition were selected. At each station, water temperature, salinity and oxygen concentration were measured by a Conductivity-Temperature-Depth profiler (CTD). Abundant species were used for respiration measurements on board while subsamples from the same populations were deep-frozen at – 80°C for subsequent enzymatic measurements conducted at the Department of Marine Zoology at the Bremen University, Germany.

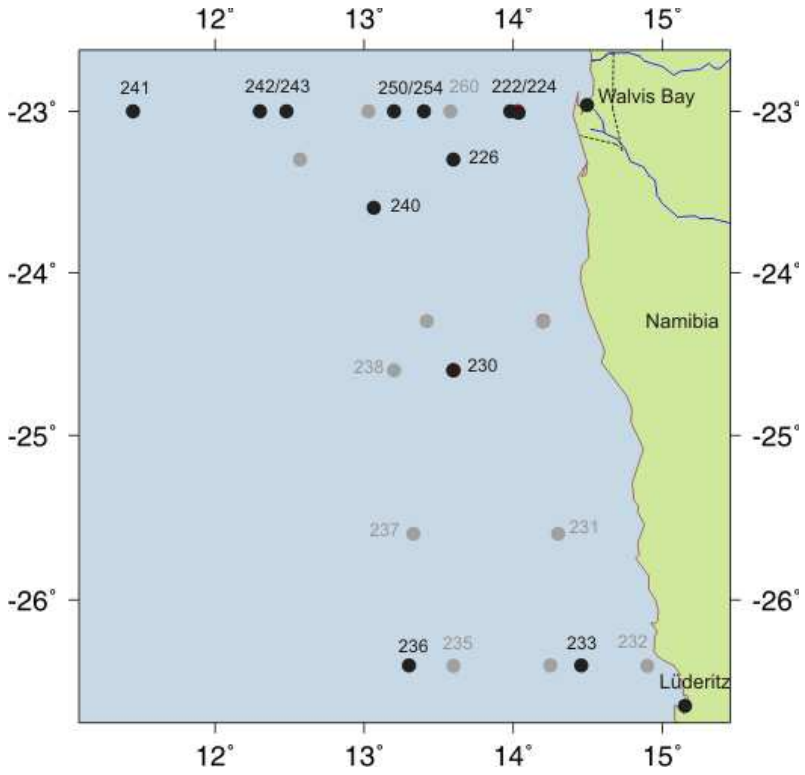

Figure 2: Station map. Black dots represent the stations where copepods were caught for this study.

2.3. Measurement of Respiration Rates of Copepod Species

2.3.1. Experimental Design

The oxygen consumption was measured using a 10-Channel Fiber-Optic Oxygen Meter (OXY-10, PreSens, Precision Sensing GmbH). The oxygen meter detects dissolved oxygen concentrations in a solution by using fiber-optic oxygen minisensors. An oxygen-sensitive foil was glued inside to ten air-tight Winkler bottles (13 ml) so that oxygen concentration could be measured non-invasively and non-destructively by the sensors from outside through the wall. The foil consists of a fluorescent dye whose collision with the oxygen molecules is detected by the sensors. Beforehand, the oxygen meter was calibrated according to the OXY-10 instruction manual.

The experiments were conducted in a temperature controlled refrigerator. For each experiment, seawater was UV treated and then oxygenated for 10 to 20 min. Afterwards it was filtered through 0.2 µm Whatman GF/F Filter to remove impurities and reduce bacterial respiration. The filtered seawater was stirred for further 10 to 20 min so that it could equilibrate its oxygen concentration to avoid supersaturation. Finally, the seawater was filled in ten Winkler bottles that had been washed with ethanol and deionized water.

In total, 20 experiments were run, of which 13 were conducted at simulated *in situ* temperatures and seven at manipulated temperatures (*in situ* temperature ± 5°C). Prior to the experiments, the copepods were kept in a second refrigerator at their respective incubation temperature for at least twelve hours to acclimatize to the conditions. Depth profiles of temperatures derived from the CTD were used to set the fridges to the ambient temperatures of the sampling depths.

In each experimental run, eight bottles were used for measurements, while two bottles were kept as controls without animals. At least four replicates were made per copepod species. The number of animals per bottle depended on the copepods' size, stage and metabolic activity (e.g. diapause) to avoid a crowding effect. For large animals as adult female *Rhincalanus nasutus*, *Eucalanus hyalinus*, *Pleuromamma robusta*, *Pleuromamma xiphias*, *Pleuromamma quadrungulata*, *Euchirella rostrata and Gaetanus pileatus*, one individual per bottle was sufficient. Small sizes had to be compensated by a larger number

of animals (2 – 3 individuals of adult females of *Calanoides carinatus*, *Candacia cheirura* and copepodite stages C4 of *R. nasutus*; 4 – 6 individuals of adult females of *Nannocalanus minor, Metridia lucens*, *Aetideus armatus* and copepodite stages C2/3 of *R. nasutus*; 6 – 18 individuals of diapausing copepodids C5 of *C. carinatus*).

The bottles were fixed to the sensors and kept in a water bath with constant temperature in the refrigerator (Figure 3). The decrease of the oxygen concentration in each bottle was measured every 15 s and was followed on a laptop running the OXY-10 software.

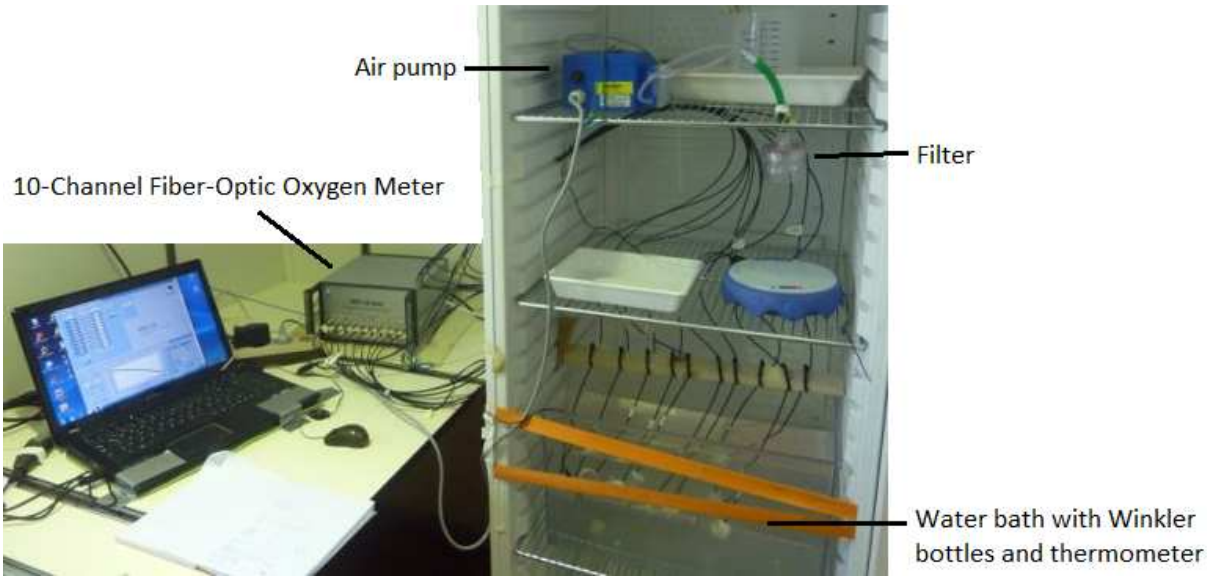

Figure 3: Experimental set-up of the 10-Channel Fiber-Optic Oxygen Meter.

2.3.2. Calculation of the Respiration Rate

The decrease of the oxygen concentration within the bottles was measured in mg O_2 per ml and plotted against time in minutes. To calculate respiration rates, the slope of declining oxygen concentration was determined, excluding at least the first hour of each experiment to reduce bias by stress and increased activity at the start of the experiment. During this time, the animals were supposed to acclimatize to the experimental conditions. The slope was then corrected for microbial respiration by subtracting the mean slope of the control bottles. The results were converted into µmol O_2 per litre using the following equation (OXY-10 manual, Precision Sensing GmbH 2005; Lampert 1984):

$$c_{O_2}[\mu mol\ min^{-1}L^{-1}] = c_{O_2}[mg\ min^{-1}L^{-1}] \times 31.25$$

The values were then converted into µmol O_2 consumption per hour per gram dry mass:

$$c_{O_2}[\mu mol\ h^{-1}g\ DM^{-1}] = \frac{c_{O_2}[\mu mol\ L^{-1}min^{-1}] \times V \times 60}{g\ DM}$$

V = volume of each bottle (L)

60 = converts minutes to hours

DM = sample dry mass in gram

To finally compare ETS-activity and respiration rate, the respiration rate was converted into µmol oxygen consumption per hour per individual:

$$c_{O_2}[\mu mol\ h^{-1}\ Ind^{-1}] = \frac{c_{O_2}[\mu mol\ L^{-1}min^{-1}] \times V \times 60}{number\ of\ individuals\ per\ bottle}$$

Calculation of Q_{10}

The Q_{10} values were calculated for females of *Metridia lucens*, *Calanoides carinatus*, *Eucalanus hyalinus*, *Pleuromamma quadrungulata* and copepodite stages C2/3 and C4 of *Rhincalanus nasutus* and C5s of *C. carinatus* to determine the change in respiration rate with temperature. An exponential regression analysis was applied. The measured respiration rates were plotted against temperature to receive an exponential equation ($y = a \times e^{b \times x}$) so that respiration rates (y) could be calculated for any temperature (x). Subsequently, the Q_{10} value was calculated as the ratio of respiration rates at temperatures 10°C apart from each other:

$$Q_{10} = \frac{R^{x+10}}{R^x}$$

R^x is the respiration rate at a certain temperature and R^{X+10} is the respiration rate at 10°C higher.

2.4. Measurement of the Respiratory Electron Transport System (ETS) Activity

2.4.1. Experimental Design

Applying an artificial electron acceptor, the electron transport system (ETS) assay is thought to estimate, under substrate saturation, the maximum activity of the key enzymes involved in the ETS: NADH dehydrogenase (complex I), Succinic dehydrogenase (complex II) and Ubiquinone (UQ) oxidoreductase (complex III) in the mitochondria and NADPH dehydrogenase in the microsomes (Packard 1971, Arístegui and Montero 1995). An overview of the ETS is given in Figure 4.

The ETS of eukaryotic cells consists of cytochromes, flavoproteins, and metallic ions that transport electrons from catabolized food to oxygen for ATP generation. The electrons enter the ETS via the flavoprotein containing NADH dehydrogenase that catalyses the transfer of two electrons to UQ. Succinic dehydrogenase delivers additional electrons from succinate at the level of coenzyme Q. Finally, UQ oxidoreductase sequentially transfers one electron from cytochrome b UQ to one molecule of cytochrome c (Hochachka and Somero 1984, Packard 1985). This cytochrome b UQ complex is the rate-limiting step within the ETS and can be measured by its reaction with 2-(p-jodophenyl)-3-(p-nitrophenyl)-5-phenyl tetrazolium chloride (INT) using NADH, NADPH and succinate as electron donors (Chance 1954, Chance et al. 1955, Packard 1971).

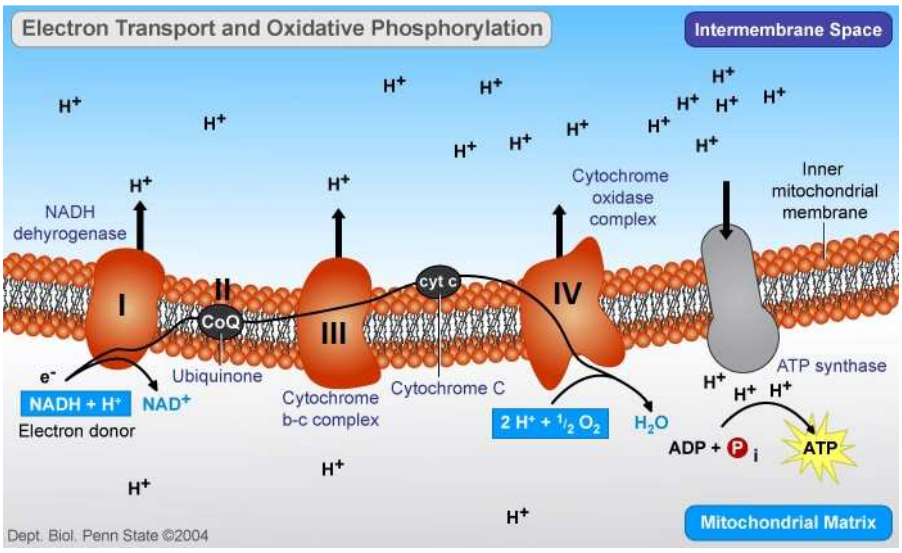

Figure 4: Overview of the mitochondrial electron transport system showing complex I – III which are involved in the ETS-assay.

The yellow coloured tetrazolium salt serves as an artificial electron acceptor and is reduced to reddish coloured formazan that has its absorption maximum at 490 nm and can be detected photometrically (Kenner and Ahmed 1975). For ETS measurements animals of the same populations, of which also respiration rates had been measured, were used. In total, ETS-activities of nine species were measured: *Eucalanus hyalinus* (f), *Rhincalanus nasutus* (f, C4, C2/3), *Pleruomamma xiphias* (f), *Pleuromamma robusta* (f), *Pleuromamma quadrungulata* (f), *Calanoides carinatus* (f, C5*), Nannocalanus minor* (f), *Aetideus armatus* (f) and *Metridia lucens* (f). The method of Packard (1971) modified by Owens and King (1975) was applied and optimized for the species used in the experiments.

All chemicals were ordered at Merck Group, except for INT which was ordered at Sigma Aldrich (Fluka). NADH, NADPH and INT were wrapped in aluminium foil to avoid light exposure and stored in a refrigerator at +2 to +8°C, along with the prepared reaction solutions:

Phosphate buffer (0.1 M)

Phosphate buffer was prepared in 600 ml portions, whereas a) 0.591 g monohydric sodium dihydrogen phosphate (NaH_2PO_4*H_2O) was added to 20 ml of deionized water (dH_2O) and b) 8.52 g anhydrous disodium hydrogen phosphate (Na_2HPO_4) were added to 300 ml dH_2O. 16 ml of a) and 284 ml of b) were mixed and filled up to 600 ml to obtain pH 8. The pH was regulated to 8.1 by adding dropwise 1 M Sodium hydroxide (NaOH). 1.2 ml (0.2 % v/v) Triton X-100 were added. Triton X-100 acts as a detergent that brings the insoluble formazan into solution (Owns and King 1975).

Homogenizing buffer

To preserve ETS enzyme activity, 3.697 mg Magnesium sulfate heptahydrate (75 µM, $MgSO_4$ x 7 H_2O) and 100 mg Polyvinylpyrrolidone (0.5 mg/ml, PVP) were added to 200 ml stock buffer (Packard 1971, Table 1). 50 ml were stored in a refrigerator for immediate usage, the rest was frozen at – 20°C in 50 ml portions.

Table 1: Dependence of ETS-activity on different PVP concentrations in the homogenizing buffer using an example of *Paraeuchaeta gracilis*. The difference of the ETS-activities between 1.5 and 0.5 mg PVP ml^{-1} was significant (Mann Whitney test, p-value 0.03, n=4).

PVP [mg ml^{-1}]	ETS-activity [µL O_2 h^{-1}g WM^{-1}]
1.5	188 ± 17.2
0.5	297 ± 4.4
0.15	294.5 ± 4.2

Substrate buffer

Substrate buffer was prepared daily with concentrations of 1.3 mM NADH, 0.05 mM NADPH and 1 mM succinate in the appropriate volume of stock buffer (Figure 5, 6, 7). Due to the succinate, the pH had to be re-regulated to 8.1. The solution was prepared and stored on ice. When taken out of the fridge it was wrapped in aluminium foil.

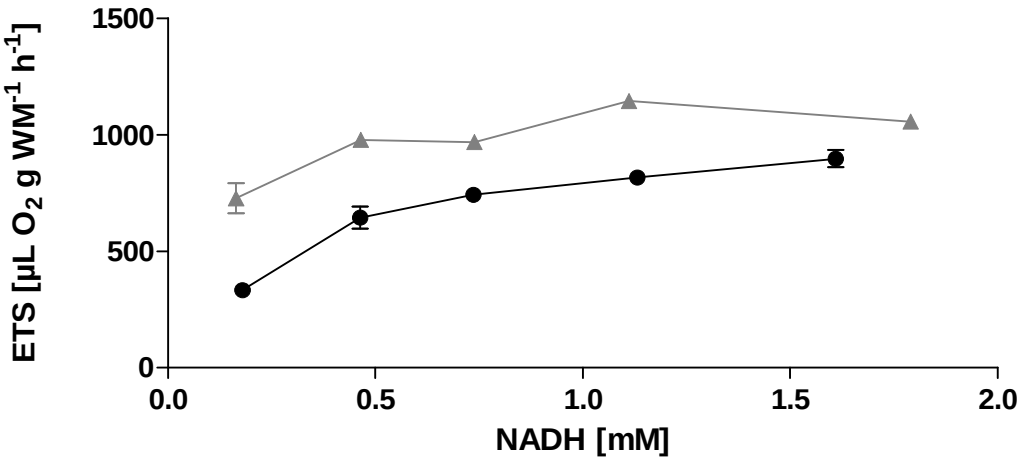

Figure 5: Saturation curve for different NADH-concentrations using an example of *Eucalanus hyalinus* (grey triangles) and *Paraeuchaeta gracilis* (black dots). Mean values and standard deviations are given (n=4).

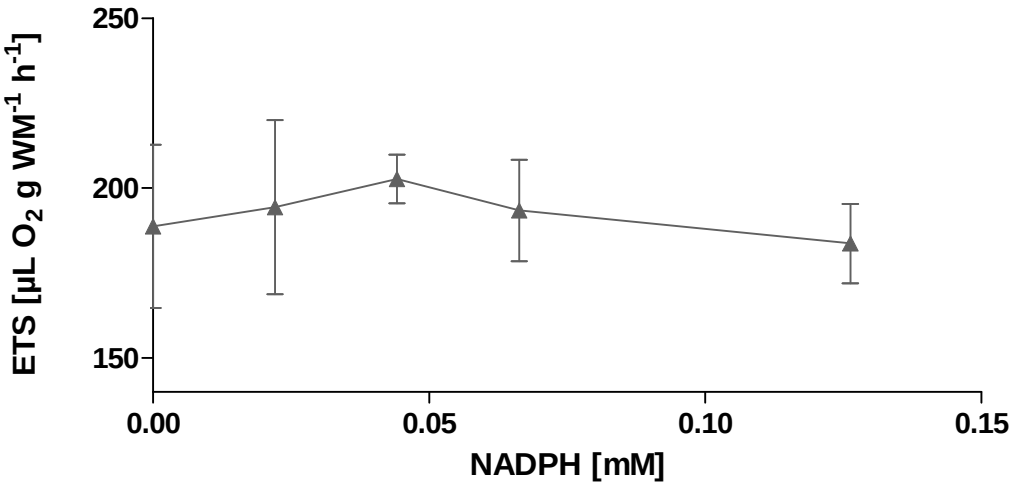

Figure 6: Saturation curve for different NADPH-concentrations using an example of *P. gracilis*. Mean values and standard deviations of are given (n=3-4).

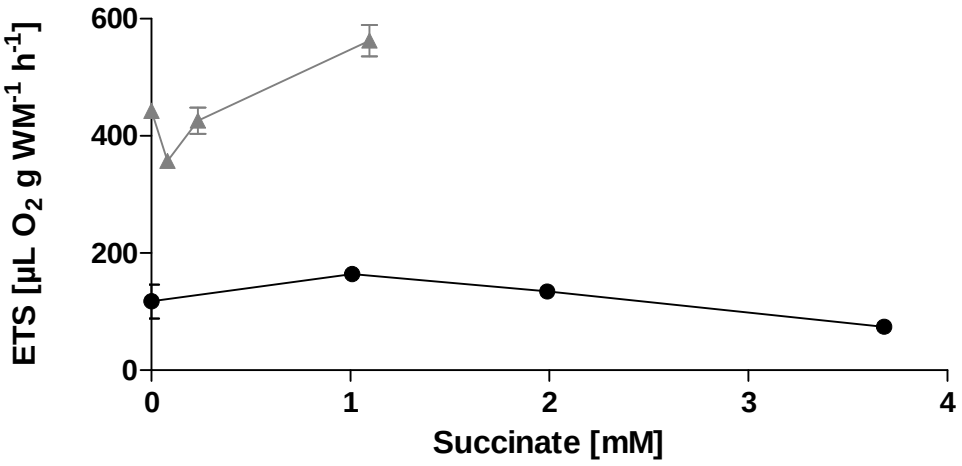

Figure 7: Saturation curve for different succinate concentrations using an example of *P. gracilis* (black dots) and *E. hyalinus* (grey triangles). Mean values and standard deviations are represented (n=4). In the test with *P. gracilis* a higher PVP concentration was used explaining the generally lower values.

INT-solution

2.5 mM INT-solution was prepared in 100 ml portions (Figure 8). 126.43 mg INT was diluted in 100 ml dH_2O (Table 2). The pH was adjusted carefully to pH 7.7 with HCl (0.1 M) and NaOH (0.1 M).

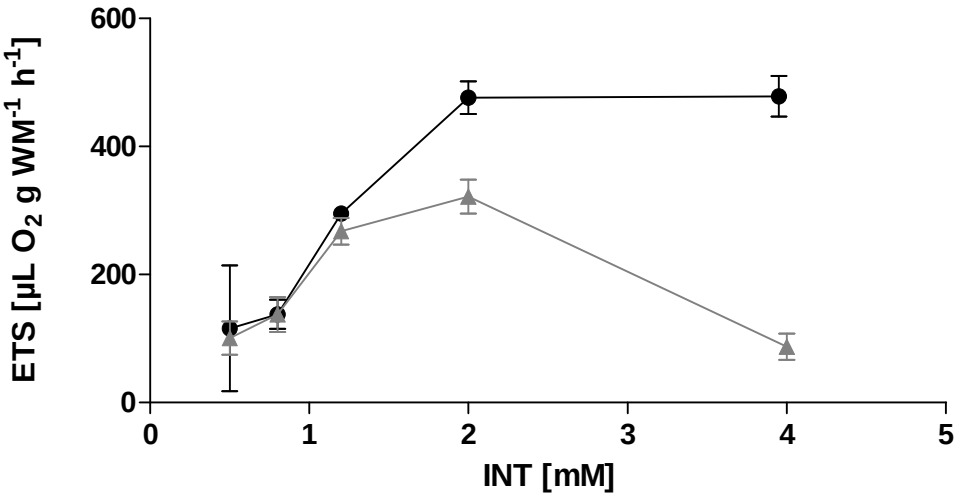

Figure 8: Saturation curve for different INT concentrations is shown using an example of *P. gracilis* (black dots) and *E. hyalinus* (grey triangles). Mean values and standard deviations are given (n=3-4).

Table 2: INT (2.5 mM) was diluted in phosphate buffer and dH_2O. Samples of *P. gracilis* were used. ETS-activities were significantly different (Mann Whitney test, p-values = 0.03, n=4). The lower range of the first two values could be explained by higher PVP concentrations.

	INT in phosphate buffer	**INT in deionized H_2O**
ETS-activity	129 ± 6.9	150 ± 9.1
[µL O_2 h^{-1}g WM^{-1}]	754 ± 21.97	866 ± 60.97

All experimental steps were conducted on ice. Care was taken with every preparatory step to minimize bacterial contamination. The pH of the INT solution had to be controlled every day (WTW pH-meter).

Prior to each experiment, the wet mass of one to five copepods per measurement (depending on the copepods' size) was measured on a Microbalance (Satorius, NC21S, precision ± 10 µg). Immediately after weighing, the copepods were transferred into a 2 ml Eppendorf cup containing 500 µL homogenizing buffer (HOM). The animals were then homogenized on ice for two minutes using a hand pistil. After homogenization, the preparation was transferred to a 15 ml centrifugation tube with two rinsing steps. HOM buffer was added to a dilution of 1:1 where maximal ETS-activities have been measured (1

mg copepod per ml HOM buffer). The homogenate was then centrifuged for ten minutes at 4700 g at 0°C and afterwards stored on ice.

600 µL substrate buffer and 200 µL INT-solution were incubated with 200 µL supernatant (3:1:1) in a 2 ml Eppendorf cup while stirred in a thermomixer (Eppendorf thermomixer comfort) at the respective *in situ* temperature of the sample. The minimum temperature of the thermomixer was 6°C which is why *P. quadrungulata* was measured at 6°C and not at its *in situ* temperature of 5°C. The reaction of each assay was started with an offset of 50 s by adding the supernatant while a stop watch was running. After a species-specific incubation time the absorbance was read in 2 ml quartz cuvettes in a tempered photometer (Kotron Instruments, UVIKON 941) at 490 nm using dH_2O as a reference (program "fixed wavelength").

To receive maximum ETS-activities, the incubation time was determined for each species by measuring the absorbance every ten minutes for a total period of 70 to 80 minutes. They varied from 20 to 70 min (Table 3).

For each measurement, three parallel samples were measured. Each sample was measured in quadruplicates accompanied by three sample blanks. Sample blanks contained 600 µL phosphate buffer, 200 µL INT-solution and 200 µL homogenate supernatant. Furthermore, a triplicate substrate blank was run daily containing 600 µL substrate solution, 200 µL INT-solution and 200 µL homogenizing buffer in order to correct the absorption of each assay for unspecific reactions.

Table 3: Incubation times for each species when ETS-activity was maximal.

Species	Stage	Incubation Time [min]
Calanoides carinatus	C5	20
Calanoides carinatus	f	40
Nannocalanus minor	f	40
Aetideus armatus	f	40
Metridia lucens	f	40
Eucalanus hyalinus	f	50
Rhincalanus nasutus	f, C2/C3, C4	50
Pleuromamma sp.	f	70

2.4.2. Calculation of the ETS-activity

ETS-activity was calculated with the following equation (Packard and Williams 1981; Simčič and Brancelj 1997):

$$ETS\ (\mu L\ O_2 h^{-1} g\ WM^{-1}) = \frac{Abs^{490}\ (corrected)\ \times\ H\ \times\ S\ \times\ 60}{1.42\ \times W\ \times\ f\ \times\ t}$$

Abs^{490} = corrected sample absorption

H = volume of the original homogenate (ml)

S = final volume of the reaction mixture (1 ml)

60 = converts the measurement to units of hours

W = wet mass of the sample (g)

f = volume of the incubated aliquot of the homogenate (0.2 ml)

t = incubation time (min)

1.42 = converts formazan production into volume O_2 (µL) (Kenner and Ahmed 1975)

The ETS-activity was then converted into µmol O_2 h^{-1}g WM^{-1} whereas the volume of dissolved oxygen of 1 ml L^{-1} equals 44.6 µmol O_2 L^{-1} (Lampert 1984, Harris et al. 2000):

$$ETS\ (\mu mol\ O_2 h^{-1} g\ WM^{-1}) = \frac{ETS\ (\mu L\ O_2 h^{-1} g\ WM^{-1})\ \times\ 44.6}{1000}$$

Since respiration rates were given in µmol oxygen per hour per gram dry mass, respiration rates and ETS-activity had to be converted to comparable units:

$$ETS\ (\mu mol\ O_2 h^{-1} Ind^{-1}) = \frac{ETS\ (\mu mol\ O_2 h^{-1} g\ WM^{-1})\ \times\ (g\ WM\ per\ sample)}{number\ of\ individuals\ per\ sample}$$

With respiration rates and ETS-activities given as oxygen consumption per individual per hour, ETS:R and R:ETS ratios were calculated.

2.5. Measurement of Lactate Dehydrogenase (LDH) Activity

2.5.1. Experimental Design

Lactate dehydrogenase (LDH) gains energy in the form of ATP when oxygen is absent. It converts pyruvate, the final product of glycolysis, to lactate with concomitant oxidation of NADH. To measure the activity of lactate dehydrogenase (LDH) within the pyruvate oxidoreductase pathway, the different absorption maxima of reduced NADH and oxidized NAD^+ are exploited during the reduction of pyruvate:

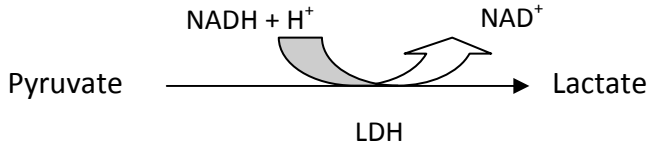

Unlike NAD^+, NADH has a second absorption maximum at 340 nm (Figure 9). When NADH is oxidized to NAD^+ the reaction can be followed photometrically at 340 nm as a decrease in absorption.

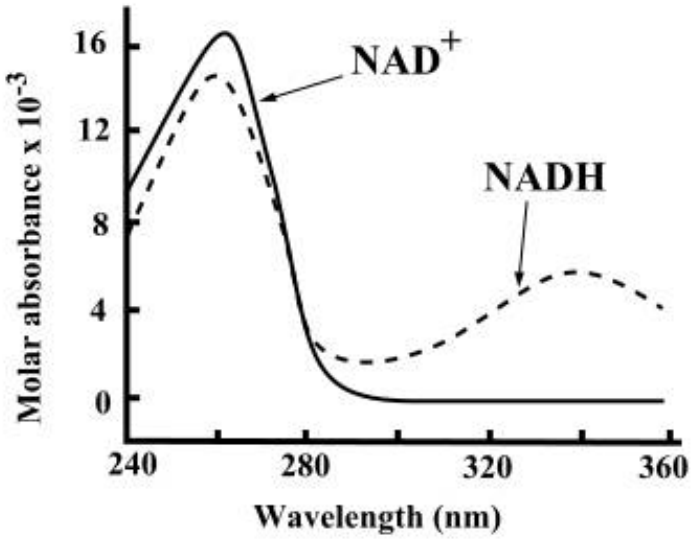

Figure 9: Oxidized NAD^+ and reduced NADH have one absorption maximum at a wavelength around 260 nm while NADH has another at 340 nm (http://de.academic.ru/pictures/).

The method was conducted after Schiedek (1997), modified by Thuesen et al. (1998) and Gonzales and Quiňones (2002). It was optimized for the species used in this study. Because some species showed maximal LDH-activity at pH 7.2 and some at pH 5.8, all

measurements were made at both pH values at 20°C. Thus, two different phosphate buffers (80 mM) were prepared, one with pH 7.2 and the other with pH 5.8. For each pH, NADH solutions (8.4 mM) and pyruvate solutions (0.984 mM) were prepared every day with an end concentration of 0.2 mM and 0.45 mM respectively within the assay mixture (Figure 10, 11). The NADH solution was shielded from light by aluminium foil and kept on ice while the pyruvate solution and phosphate buffer was brought to room temperature before measurements started.

The preparation of the homogenate was the same as for the electron transport system assay (see 2.4.1). However, a different sample dilution of 5 mg copepod per ml phosphate buffer was chosen (Figure 12). The homogenate was then centrifuged for ten minutes at 6600 g (0 – 4°C) and afterwards stored on ice.

All measurements were made in triplicates while deionized water was used as a reference. Three empty 2 ml quartz cuvettes were put into a tempered photometer which was kept at 20°C. First, 530 µL phosphate buffer, 480 µL pyruvate solution and 25 µL NADH solution were added and stirred for 15 s. Thereupon the absorption was measured every 18 s until the value was stable to minimize unspecific reactions. To start the reaction, 15 µL of the supernatant was added to each cuvette with a multi pipette and the decrease in absorption was followed for 3 min every 18 s (program “Auto rate assay”).

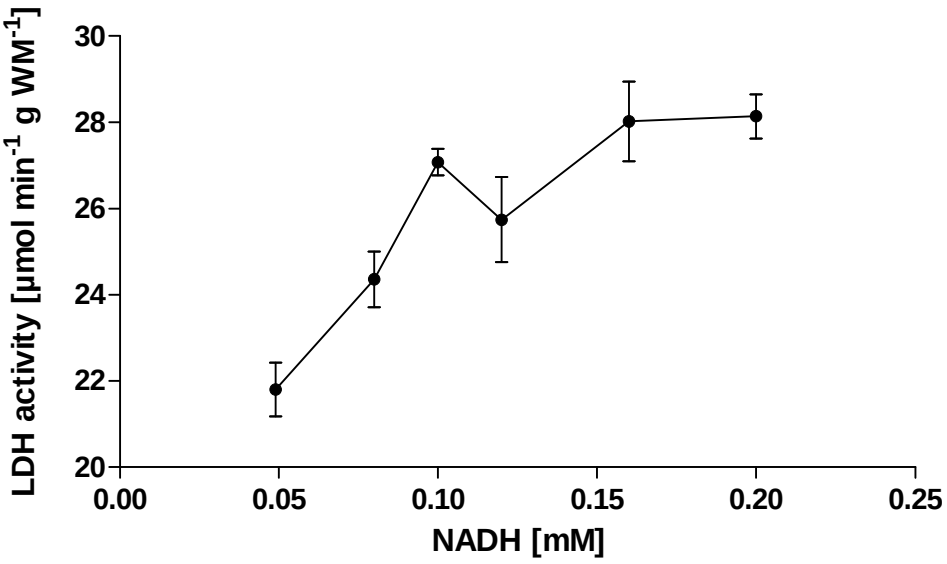

Figure 10: Saturation curve of NADH. LDH activity is plotted against end concentrations of NADH in the assay mixture. An example of *Eucalanus hyalinus* was used (n=3).

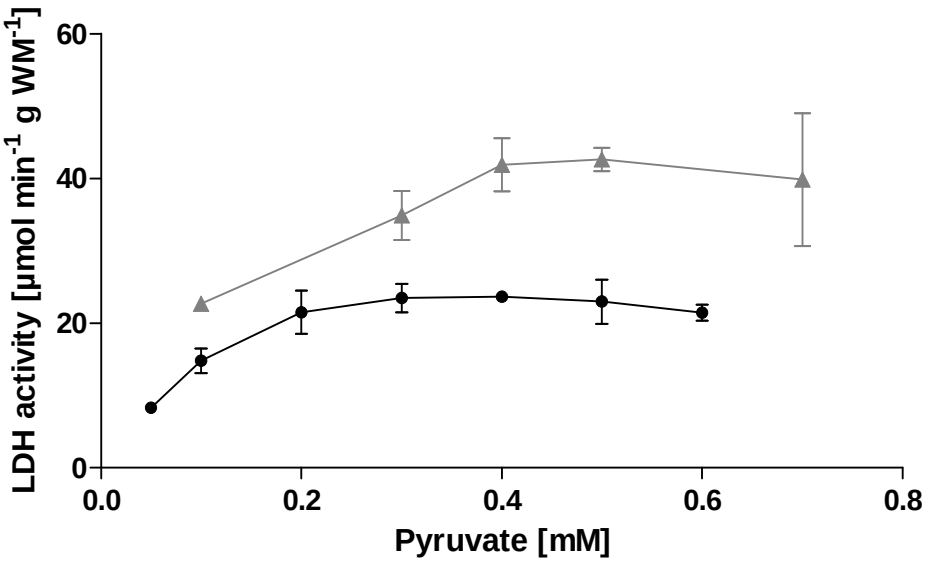

Figure 11: Saturation curve of pyruvate. LDH-activity is plotted against end concentrations of pyruvate in the assay mixture. Examples of *E. hyalinus* (back dots) and *R. nasutus* (grey triangle) are shown (n=3).

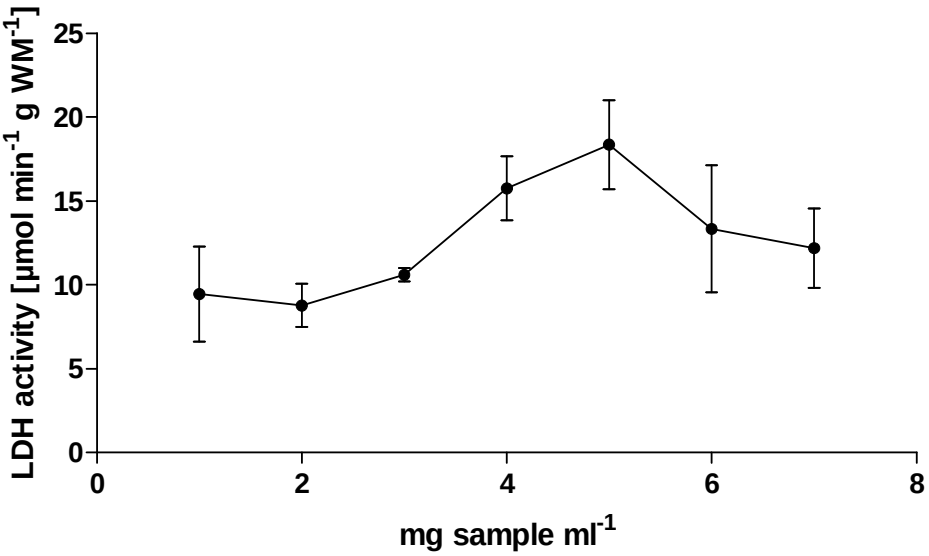

Figure 12: Dependence of LDH-activity on the sample dilution demonstrated by an example of *Pleuromamma xiphias* (n=3).

2.5.2. Calculation of the LDH-activity

Enzyme activity is expressed in units per gram wet mass (U g WM^{-1}) of the copepod, where one unit equates one µmole of substrate converted to product per minute. The mean decrease in absorption of the triplicate measurements was plotted against time in minutes. To calculate the LDH-activity, the slope of each plot was determined and the following equation was applied. It is derived from the Beer-Lambert Law that describes the relation between optical density of a solution and its concentration (Harris et al. 2000):

$$A = \varepsilon \times \mathrm{C} \times \mathrm{d}$$

$$\leftrightarrow C = \frac{A}{\varepsilon \times d}$$

$$\rightarrow \frac{\Delta A\ min^{-1}}{\varepsilon \times d} = \frac{\Delta A\ min^{-1}}{6.22 \times 10^{6} cm^{2} mol^{-1} \times 1\ cm} = (\Delta mol\ ml^{-1})\ min^{-1}$$

A = sample absorption

C = concentration of substance in mol L^{-1}

ε = molar extinction coefficient of NADH (6.22 x 10^6 cm^2 mol^{-1})

d = path length of the cuvette (1 cm)

ΔA min^{-1} = decrease in absorption per minute

The total activity of the assay mixture is calculated and converted to µmoles, where V is the final volume of the reaction mixture (1.05 ml):

$$(\Delta mol\ ml^{-1})\ min^{-1} \times V\ ml \times 10^{6} = \mu mol\ min^{-1}$$

To obtain the activity for 1 g of tissue, the dilution of the sample has to be considered. H is the original homogenate volume (ml), v the volume of the incubated aliquot of the homogenate (0.015 ml), and S the wet mass of the sample in gram:

$$(\mu mol\ min^{-1}) \times \frac{1}{v} \times \frac{H}{S} = \mu mol\ min^{-1} g\ wwt^{-1}$$

In summary, the following equation results when 10^6 can be cancelled:

$$U\ g\ WM^{-1} = \mu mol\ substrate\ min^{-1} g\ WM^{-1} = \frac{\Delta A\ min^{-1} \times V \times H}{\varepsilon \times d \times v \times S}$$

2.6. Data Analysis

Allometric Relationships

Allometric relationships between metabolic rates and body mass are usually expressed as $Y = a\,W^b$ (Hochachka and Somero 2002). In this case Y is the respiration or ETS-activity, W the dry or wet mass in milligram, a the normalization constant and b the scaling coefficient. Another way to express this relationship is: $\log(Y) = \log(a) + b \times \log(W)$. The metabolic rates were plotted log transformed against log body mass. Applying linear regression analysis, b is received as the slope of the line and a the intercept.

Multiple regression analysis was applied to analyse the correlation between metabolic rates, body mass and temperature. Either respiration rate or ETS-activity was chosen as the dependent variable Y while the two independent variables X_1 and X_2 represented each body mass and temperature. The parameters are the coefficients β_0, β_1, and β_2 where β_0 is the Y-intercept and β_1 and β_2 the slopes:

$$\log(Y) = \beta_0 + \beta_1 \times \log(X_1) + \beta_2 \times X_2$$

Statistical Analysis

An unpaired t-test assuming equal variance was conducted to test the metabolic rates for significant differences. If conditions for normality were either not met or could not be tested because of too few replicates, the non-parametric Mann-Whitney test was performed. To compare more than two means, one-way ANOVA assuming equal variance or the non-parametric Kruskal-Vallis test assuming no Gaussian distribution was adopted. The null hypothesis H_0 assumes that groups are taken from the same population and do not differ. H_0 is accepted if the p-value is larger than 0.05. On the other hand, it is rejected if the p-value is less than 0.05. To analyse the effect of different temperatures on the respiration rates, respiration rates were log transformed and plotted against temperature to perform linear regression analyses.

3. Results

3.1. Hydrographic Regime

Sea surface temperature (SST), salinity and Chlorophyll a concentrations during the cruise are illustrated in Figure 13. Typical vertical profiles of oxygen and temperature are shown in Figure 14 (for the location of the stations see Figure 2).

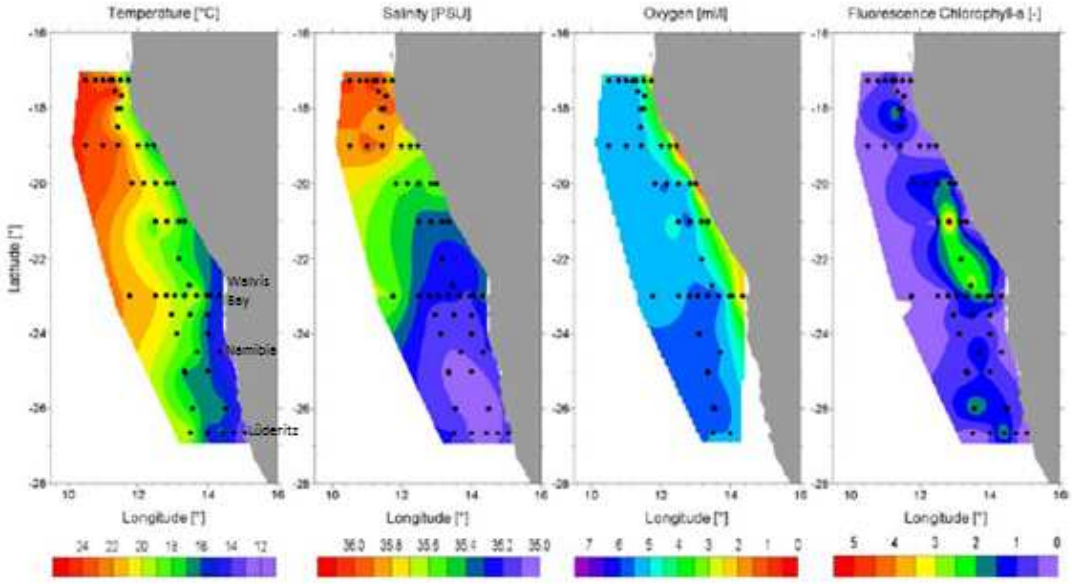

Figure 13: Horizontal distribution of temperature, salinity, oxygen and chlorophyll a fluorescence off Namibia at 20 m depth during the MSM17/3 cruise (based on CTD data, Mohrholz et al. 2011).

Salinity was more or less constant. At the Walvis Bay transect, the sea surface temperature ranged from 22°C at the open ocean (Stn241) to around 18°C (Stn222) near the continent indicating only weak to no active upwelling when samples were taken. Figure 13 shows mean values over 26 days which is why upwelling appears stronger. A thermocline between 10 m and 40 m was most pronounced at station 241 where temperatures dropped from 22°C to 16°C. Oxygen concentrations at the sea surface were 2 and 3 ml L^{-1} near the coast and rose to 5 to 6 ml L^{-1} in the open ocean. At station 260 and 254, oxygen concentrations dropped below 1.4 ml L^{-1} beneath 75 m and 110 m, respectively. A narrow intermediate oxygen minimum layer (IOML) was observed between 220 and 300 m at

station 250. At the Lüdertiz transect, temperatures increased from the continental shelf region from 12 to 13°C (Stn231) to around 20°C in the open ocean (Stn236) indicating strong coastal upwelling. A thermocline was observed between 30 m and 50 m. Surface oxygen concentrations varied between 5 ml L^{-1} and 6 ml L^{-1}.

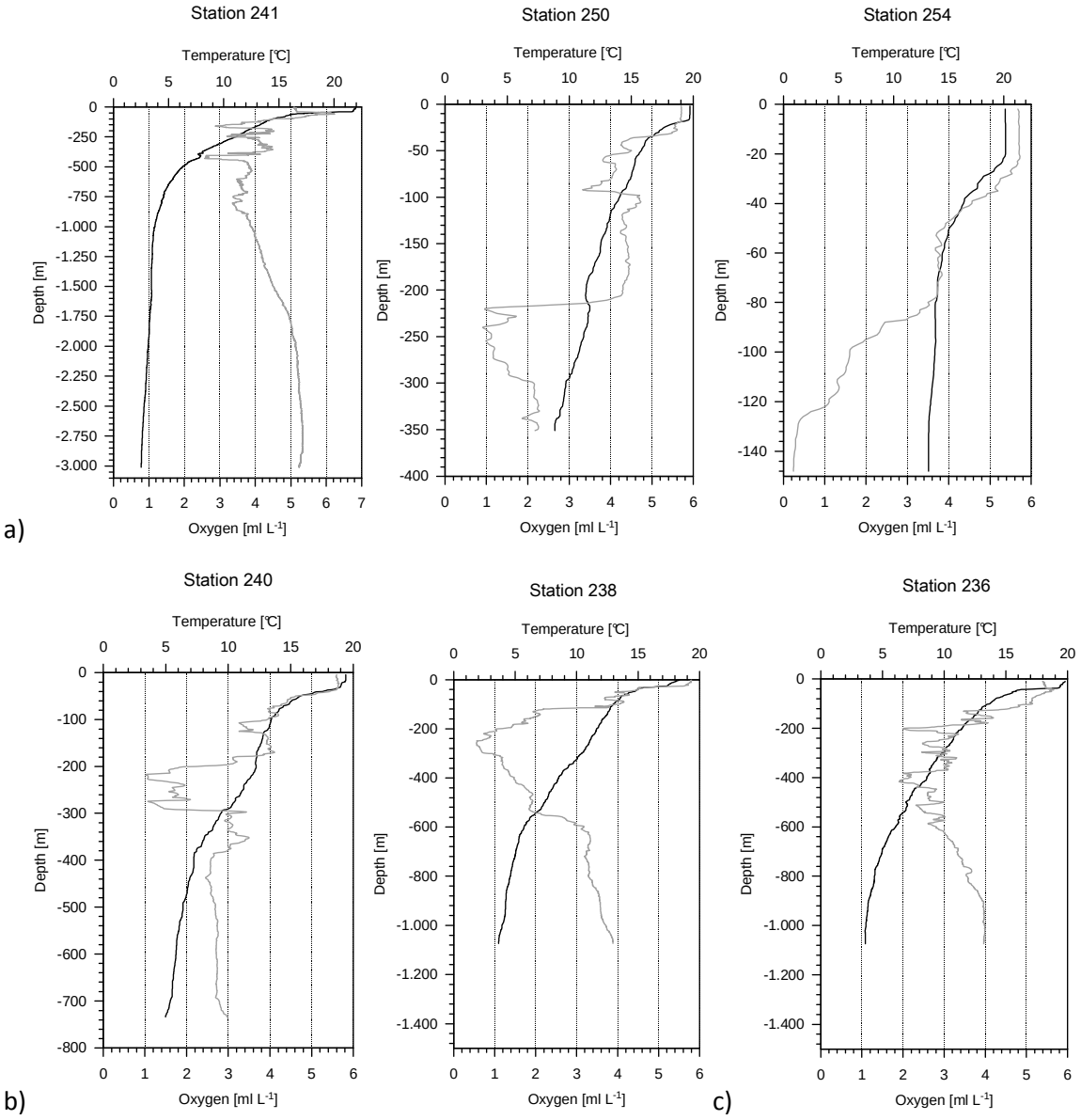

Figure 14: Typical depth profiles of temperature (black lines) and oxygen (grey lines) of a) the Walvis Bay transect, b) two stations in between the transects and c) the Lüderitz transect (CTD data were taken from Mohrholz et al. 2011).

3.2. Respiration Rates of Copepods

3.2.1. Respiration Rates at Habitat Temperatures

Respiration rates at ambient temperatures were determined for twelve copepod species and varied from 17 to 157 µmol 0_2 h^{-1} g DM^{-1} and 0.003 to 0.061 µmol 0_2 h^{-1} Ind^{-1} (Table 4). If not further specified, the species mentioned concern adult females. It was not possible to differentiate between copepodids C2 or C3 of *Rhincalanus nasutus*.

Mass-specific Respiration

Between 5 to 10°C the respiration rates varied from 17 to 99 µmol 0_2 h^{-1} g DM^{-1}. The highest mean mass-specific respiration rate was measured in medium-sized *Pleuromamma robusta*. *P. robusta* from 400 – 200 m showed a significantly higher respiration rate (99 ± 32 µmol 0_2 h^{-1} g DM^{-1}) than *P. robusta* from 600 – 400 m (71 ± 11 µmol 0_2 h^{-1} g DM^{-1}) (p-value = 0.03). The larger copepods *Pleuromamma quadrungulata* (50 ± 5 µmol 0_2 h^{-1} g DM^{-1}) and *Pleuromamma xiphias* (48 ± 11 µmol 0_2 h^{-1} g DM^{-1}) showed significantly lower oxygen consumption rates (p-values < 0.05). The lowest respiration rate was measured in the second largest copepod *Eucalanus hyalinus* (17 ± 13 µmol 0_2 h^{-1} g DM^{-1}) while the largest copepod *Geatanus pileatus* had a respiration rate of 35 ± 4 µmol 0_2 h^{-1} g DM^{-1}.
Between 13 to 16°C the mass-specific respiration rates ranged from 45 to 157 µmol 0_2 h^{-1} g DM^{-1}. The highest rate was measured in the small copepod *Aetideus armatus* (157 ± 19 µmol 0_2 h^{-1} g DM^{-1}). Furthermore, high respiration rates of 147 ± 59 µmol 0_2 h^{-1} g DM^{-1} and 140 ± 26 µmol 0_2 h^{-1} g DM^{-1} were measured in small-sized females of *Calanoides carinatus* and *Metridia lucens*, respectively. *E. hyalinus* had comparably low mass-specific respiration rates (86 ± 34 µmol 0_2 h^{-1} g DM^{-1}) while comparably smaller-sized copepodite stages C4 and females of *R. nasutus* had the lowest rates (45 ± 18 µmol 0_2 h^{-1} g DM^{-1}, 37 ± 24 µmol 0_2 h^{-1} g DM^{-1}).

Individual Respiration

Between 5 and 10°C the individual respiration rates varied from 0.003 to 0.046 µmol 0_2 h^{-1} Ind^{-1}. *Geatanus pileatus* had the highest individual respiration rate (0.046 ± 0.006 µmol 0_2 h^{-1} Ind^{-1}), followed by *P. xiphias* (0.031 ± 0.006 µmol 0_2 h^{-1} Ind^{-1}), *P. robusta* (0.035 ± 0.01 and 0.027 ± 0.007 µmol 0_2 h^{-1} Ind^{-1}) and *P. quadrungulata* (0.025 ± 0.001 µmol 0_2 h^{-1} Ind^{-1}). The lowest individual respiration rate was measured in small-sized diapausing C5s of *C. carinatus* (0.005 ± 0.001 µmol 0_2 h^{-1} Ind^{-1}).

From 13 to 16°C individual respiration rates ranged from 0.008 to 0.061 µmol 0_2 h^{-1} Ind^{-1} whereas *E. hyalinus* showed the highest individual respiration rate (0.061 ± 0.021 µmol 0_2 h^{-1} Ind^{-1}). The lowest individual respiration rates were measured in the smallest copepods as copepodids C4 (0.003 ± 0.0015 µmol 0_2 h^{-1} Ind^{-1}) and C2/3 of *R. nasutus* (0.003 ± 0.001 µmol 0_2 h^{-1} Ind^{-1}) and *M. Lucens* (0.008 ± 0.001 µmol 0_2 h^{-1} Ind^{-1}).

Table 4: Individual and dry mass-specific respiration (mean ± SD) rates of twelve copepod species at respective simulated *in situ* temperatures. Stations, sampling depths, dry masses and number of replicates (n) are given.

Species	Stage	Station	Sampling depth [m]	T [°C]	Dry Mass [µg Ind^{-1}]	Respiration rate		n
						[µmol O_2 h^{-1} g DM^{-1}]	[µmol O_2 h^{-1} Ind^{-1}]	
Aetideus armatus	f	254	100 – 50	15	84 ± 7	157 ± 19	0.013 ± 0.0013	4
Calanoides carinatus	f	224	75 – 50	13	98 ± 7	147 ± 59	0.015 ± 0.006	4
Metridia lucens	f	222	100 – 50	13	56 ± 9	140 ± 26	0.008 ± 0.001	4
Candacia cheirura	f	254	100 – 50	15	112 ± 26	126 ± 7	0.015 ± 0.002	3
Nannocalanus minor	f	250	100 – 50	15	96 ± 7	119 ± 41	0.012 ± 0.004	4
Pleuromamma robusta	f	236	400 - 200	8	363 ± 26	99 ± 32	0.035 ± 0.010	4
Rhincalanus nasutus	C2/3	233	50 - 25	13	27 ± 13	97 ± 23	0.003 ± 0.001	4
Eucalanus hyalinus	f	226	50 – 25	16	862 ± 153	86 ± 34	0.061 ± 0.021	5
Pleuromamma robusta	f	236	600 - 400	8	427 ± 152	71 ± 11	0.027 ± 0.007	9
Pleuromamma quadrungulata	f	243	800 – 600	5	508 ± 48	50 ± 5	0.025 ± 0.001	5
Pleuromamma xiphias	f	242	600 – 400	7	644 ± 33	48 ± 11	0.031 ± 0.006	8
Rhincalanus nasutus	C4	233	50 – 25	13	76 ± 10	45 ± 18	0.003 ± 0.002	4
Calanoides carinatus	C5	236	600 – 400	8	125 ± 28	43 ± 12	0.005 ± 0.001	8
Rhincalanus nasutus	f	230	90 – 40	13	364 ± 110	37 ± 24	0.013 ± 0.010	5
Geatanus pileatus	f	241	600 – 400	7	1351 ± 293	35 ± 4	0.046 ± 0.006	3
Euchirella rostrata	f	242	400 – 200	10	479 ± 52	31 ± 5	0.015 ± 0.001	8
Eucalanus hyalinus	f	240	400 – 300	8	1051 ± 192	17 ± 13	0.019 ± 0.015	4

3.2.2. Effect of Temperature on Respiration Rates

The respiration rates of six copepod species, which have been used for the ambient temperature experiments, were measured additionally at different temperatures. The oxygen consumption increased with increasing temperatures (Table 5) while the differences between the respiration rates at the three different temperatures were significant within all species (Kruskal-Wallis test, p-values < 0.05). Log transformed respiration rates of the temperature shift experiments were plotted against temperature to perform linear regression analyses (Figure 15, 16). Beforehand, the species were grouped into a) large (1259 – 657 µg), b) middle (554 –352 µg) and c) small (193 – 13 µg) sized categories based on their dry mass to exclude the body mass effect. Group a) consisted of *Eucalanus hyalinus*, group b) comprised *Pleuromamma quadrungulata,* whereas group c) consisted of copepodids C2/3 and C4 *Rhincalanus nasutus*, C5s and females of *Calanoides carinatus* and *Metridia lucens*. All slopes were significantly different from zero (p-values < 0.05).

Q_{10} values were calculated using the mass-specific respiration rates (Table 5). Females of *E. hyalinus* as well as copepodite stages C2/3 and C4 of *R. nasutus* had the highest Q_{10} values between 6.1 and 6.8, whereas the Q_{10} of *P. quadrungulata* and *M. lucens* were 2 and 3.7, respectively. In three Winkler bottles with copepodids C2/3 and C4 of *R. nasutus* no respiration rates could be detected at 8°C. The effect of temperature shifts on the respiration rate in *C. carinatus* is shown in Figure 17. The Q_{10} of copepodite stage C5 of *C. carinatus* was lower than the one of adult females of *C. carinatus* (3.5 and 5.5, respectively).

Table 5: Individual and dry mass-specific respiration rates of six copepod species at three different temperatures. Means of dry mass and respiration rates are given with standard deviation (± SD). The number of replicates (n) is shown in parentheses which accounts for individual and mass-specific rates. The Q_{10} value was calculated from mass-specific respiration rates.

Species	Stage	Dry mass [µg Ind^{-1}]	Respiration Rate 5°C		10°C		15°C		Q_{10}
			µmol O_2 h^{-1}g DM^{-1}	µmol O_2 h^{-1}Ind^{-1}	µmol O_2 h^{-1}g DM^{-1}	µmol O_2 h^{-1}Ind^{-1}	µmol O_2 h^{-1}g DM^{-1}	µmol O_2 h^{-1}Ind^{-1}	
Pleuromamma quadrungulata	f	487 ± 18	50 ± 5 (5)	0.025 ± 0.001	77 ± 9 (4)	0.037 ± 0.002	98 ± 4 (4)	0.047 ± 0.010	2

			Respiration Rate 8°C		13°C		18°C		
			µmol O_2 h^{-1}g DM^{-1}	µmol O_2 h^{-1}Ind^{-1}	µmol O_2 h^{-1}g DM^{-1}	µmol O_2 h^{-1}Ind^{-1}	µmol O_2 h^{-1}g DM^{-1}	µmol O_2 h^{-1}Ind^{-1}	
Eucalanus hyalinus	f	916 ± 185	17 ± 13 (4)	0.019 ± 0.015	42 ± 20 (4)	0.041 ± 0.019	89 ± 23 (3)	0.064 ± 0.020	6.1
Calanoides carinatus	C5	112 ± 12	43 ± 12 (8)	0.005 ± 0.001	101 ± 44 (4)	0.01 ± 0.005	105 ± 22 (4)	0.015 ± 0.008	3.5
Rhincalanus nasutus	C2/3	28 ± 2	62 ± 32 (3)	0.002 ± 0.001	97 ± 23 (4)	0.003 ± 0.002	326 ± 24 (3)	0.010 ± 0.002	6.8
Rhincalanus nasutus	C4	90 ± 42	44 ± 10 (2)	0.003± 0.001	45 ± 7.5 (4)	0.003 ± 0.001	226 ± 44 (4)	0.030 ± 0.008	6.5

			Respiration Rate 9°C		13°C		19°C		
			µmol O_2 h^{-1}g DM^{-1}	µmol O_2 h^{-1}Ind^{-1}	µmol O_2 h^{-1}g DM^{-1}	µmol O_2 h^{-1}Ind^{-1}	µmol O_2 h^{-1}g DM^{-1}	µmol O_2 h^{-1}Ind^{-1}	
Calanoides carinatus	f	90 ± 10	69 ± 39 (4)	0.007 ± 0.005	147 ± 59 (4)	0.015 ± 0.006	304 ± 101 (4)	0.023 ± 0.006	5.5
Metridia lucens	f	46 ± 11	105 ± 16 (4)	0.005 ± 0.001	140 ± 26 (4)	0.008 ± 0.001	388 ± 84 (4)	0.013± 0.003	3.7

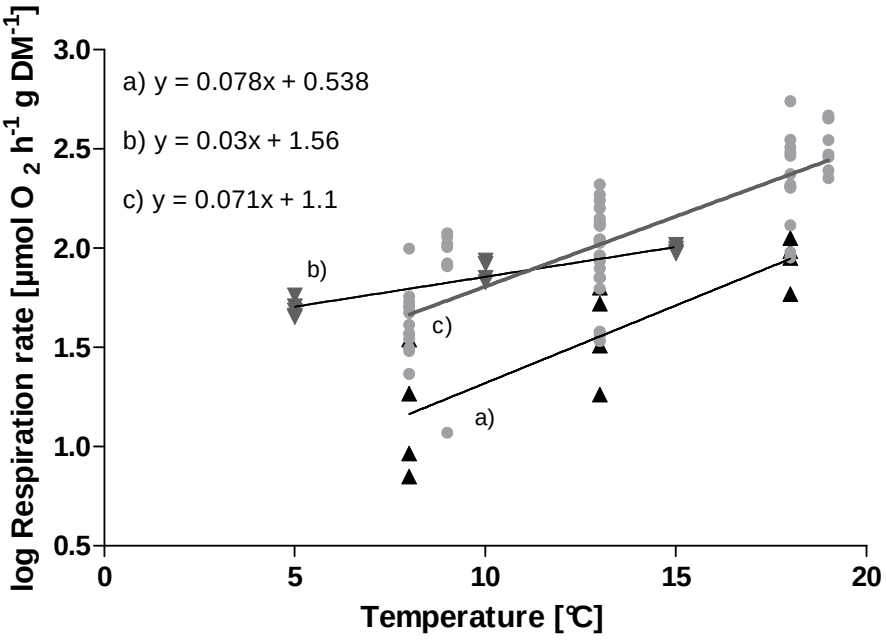

Figure 15: Log transformed mass-specific respiration rates of the temperature shift experiments, grouped into size classes a) 1259 – 657 µg (triangles), b) 554- 352 µg (reversed triangles) and c) 193-13 µg (dots), are plotted against temperature. For a) $r^2 = 0.71$, p-value = 0.0006, b) $r^2 = 0.9$, p-value < 0.0001 and c) $r^2 = 0.63$, p-value < 0.0001.

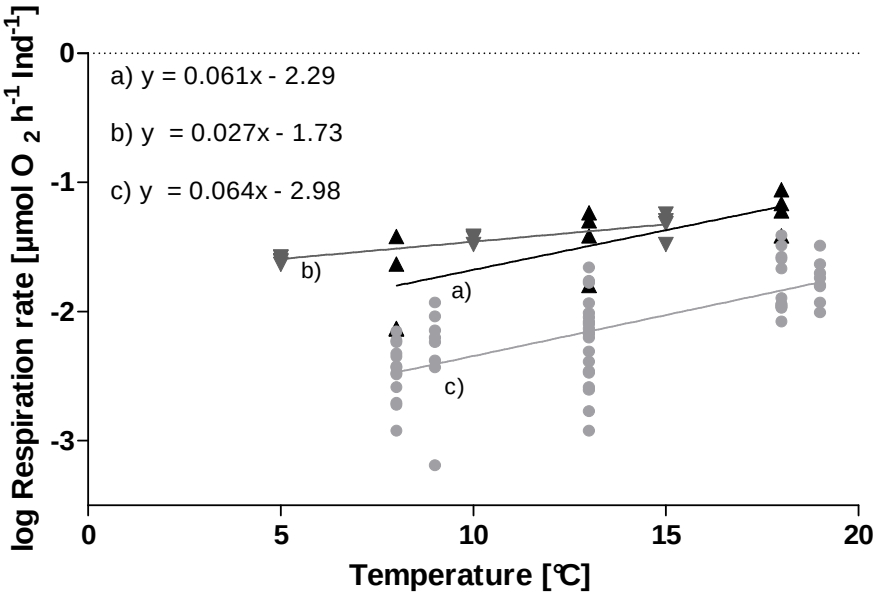

Figure 16: Log transformed individual respiration rates of the temperature shift experiments, grouped into size classes a) 1259 – 657 µg (triangles), b) 554- 352 µg (reversed triangles) and c) 193-13 µg (dots), are plotted against temperature. For a) $r^2 = 0.53$, p-value = 0.0072, b) $r^2 = 0.8$, p-value < 0.0001 and c) $r^2 = 0.47$, p-value < 0.0001.

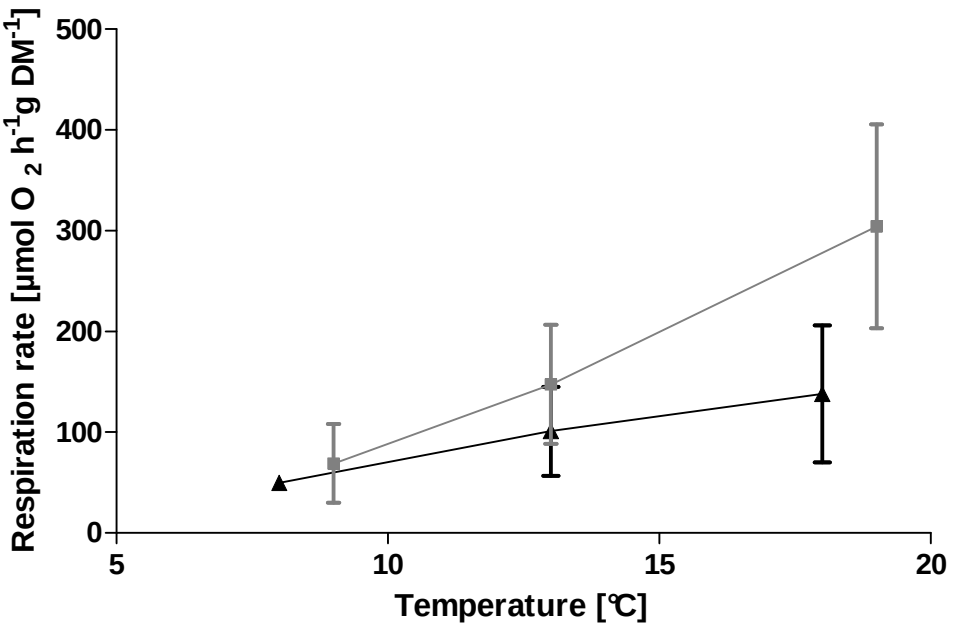

Figure 17: Mass-specific respiration rates at three different temperatures of copepodids C5 (triangles) and females (squares) of *C. carinatus* (n=4) collected at sampling depth of 600-400 m and 70-50 m, respectively.

3.2.3. Effect of Body Mass on Respiration Rates

Mass-specific respiration rates showed a decline with increasing body mass of the specimens, whereas individual respiration rates increased with copepod size (Figure 18, 19). To exclude the effect of temperature the respiration rates were grouped in two categories a) 5-10°C and b) 13-16°C. Only respiration rates measured at simulated *in situ* temperatures were used. All slopes were significantly different from zero (p-values < 0.05). In both plots the slopes were not significantly different from each other (p-values > 0.05) while the Y-intercepts differed significantly (p-value < 0.05) due to the generally higher rates measured at higher temperatures. The respiration rates were highly scattered with low coefficients of determination.

Mass-specific Respiration Rates

Between 5 and 10°C, the highest respiration rates were exhibited by *Pleuromamma robusta* (> 70 µmol O_2 h^{-1} g DM^{-1}). The lowest respiration rates (< 40 µmol O_2 h^{-1} g DM^{-1}) were measured *Eucalanus hyalinus*, *Euchirella rostrata*, *Geatanus pileatus* and copepodids C5 of *C. carinatus* but also *P. quadrungulata*, and *P. xiphias* were among them (Figure 18). Between 13 and 16°C, respiration rates higher than 100 µmol O_2 h^{-1} g DM^{-1} were measured in adult females of *C. carinatus*, *Metridia lucens*, *Aetideus armatus*, *Nannocalnus minor*, *Candacia cheirura*, and one copepodids C2/3 of *Rhincalanus nasutus*. Oxygen consumption rates lower than 100 µmol O_2 h^{-1} g DM^{-1} were detected in *E. hyalinus*, copepodids C2/3, C4 and females of *R. nasutus*, as well as one female of *C. carinatus* and *N. ninor*. For mass-specific respiration rates the following allometric equations were derived:

$$\text{Group A: } Y(\mu mol\ O_2 h^{-1} g\ DM^{-1}) = 37\ W^{-0.233}$$

$$\text{Group B: } Y(\mu mol\ O_2 h^{-1} g\ DM^{-1}) = 50\ W^{-0.258}$$

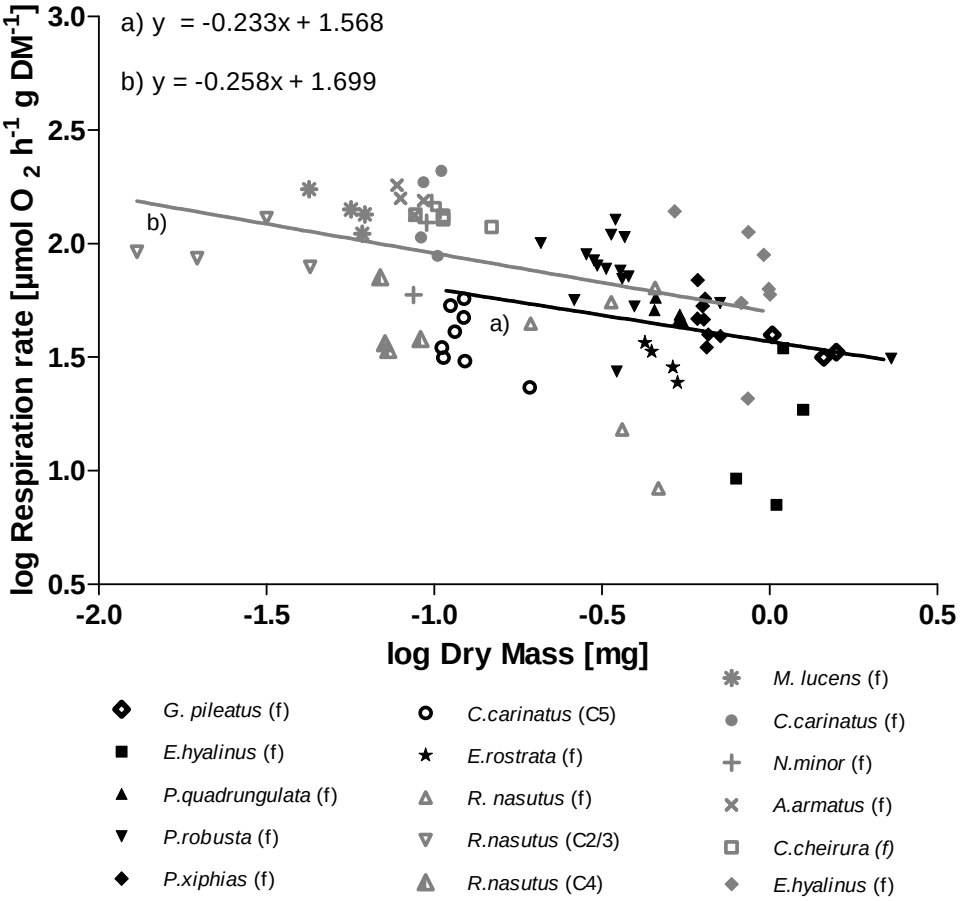

Figure 18: Correlation between log mass-specific respiration rates and log dry mass (all specimens of all species) categorized in a) 5-10°C (black symbols) and b) 13-16°C (grey symbols). Equations of the linear regression analysis are shown. For a) $r^2 = 0.09$, p-value = 0.032 and b) $r^2 = 0.16$, p-value = 0.0097. To differentiate the species, each species was given a symbol explained in the legend beneath the graph

Individual Respiration Rates

Between 5 and 10°C, the highest respiration rates (> 0.02 µmol O_2 h^{-1} Ind^{-1}) were measured in *G. pileatus*, *P. robusta*, *P. quadrungulata*, *P. xiphias* and one individual of *E. hyalinus,* while the lowest rates (< 0.01 µmol O_2 h^{-1} Ind^{-1}) were measured in copepodite stages C5 of *C. carinatus* and females of *E. hyalinus* (Figure 19).

Between 13 and 16°C, the highest respiration rates were measured in *E. hyalinus* and one female of *R. nasutus* and *C. carinatus*. The lowest respiration rates were exhibited by

copepodids C2/3 and C4 of *R. nasutus*, females of *M. lucens*, *C. carinatus*, *R. nasutus* and one *N. minor*. For individual respiration rates the following allometric equations were derived:

$$\text{Group A: } Y(\mu mol\ O_2 h^{-1} Ind^{-1}) = 0.037\ W^{0.761}$$

$$\text{Group B: } Y(\mu mol\ O_2 h^{-1} Ind^{-1}) = 0.049\ W^{0.74}$$

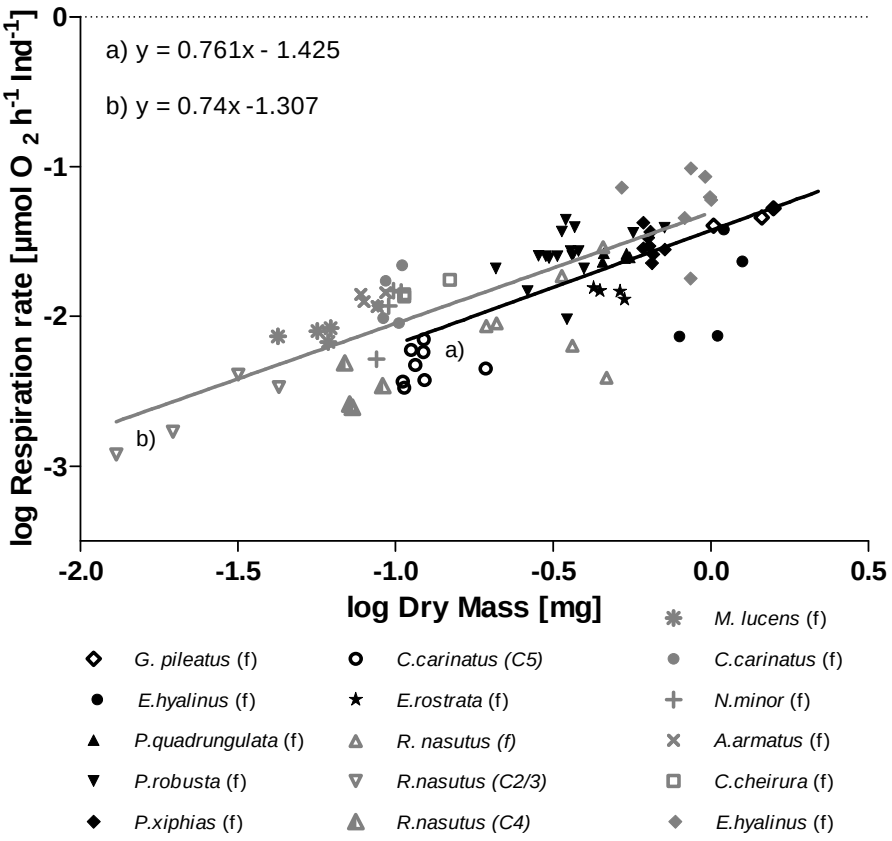

Figure 19: Correlation between log individual respiration rates and log body mass (all specimens of all species) categorized in a) 5-10°C (black symbols) and b) 13-16°C (grey symbols). Equations of linear regression analysis are shown (a) $r^2 = 0.525$, b) $r^2 = 0.628$, p-values < 0.0001). To differentiate the species, each species was given a symbol explained in the legend beneath the graph

Dependence of Respiration Rates on Dry Mass and Temperature

A model was developed for predictive purposes of the copepods' respiration rates at their habitat temperatures (Figure 20). Copepodids C5 of *Calanoides carinatus* were excluded because it was assumed that diapausing animals react differently than active ones (Ikeda et al. 2001). The best fit was received with the model containing all experimental temperatures. In both models, the influence of the dry mass and temperature on respiration was statistically significant (p-values < 0.0001). 50.8% of the variance of the mass-specific respiration rates was explainable by body mass and temperature (r = 0.712, r^2 = 0.508). The following equation was derived, where X_1 is the copepods' dry mass expressed in mg and X_2 the temperature in °C:

$$Log(Y\ \mu mol\ O_2 h^{-1} g\ DM^{-1}) = \log(16) - 0.272 \times \log(X_1) + 0.04 \times X_2$$

Contrarily, 66.6% of the variance of individual respiration rates could be explained by dry mass and temperature (r = 0.816, r^2 = 0.666). The following equation was derived:

$$Log(Y \mu mol\ O_2 h^{-1} Ind^{-1}) = \log(0.016) + 0.728\ \times \log(X_1) + 0.04 \times X_2$$

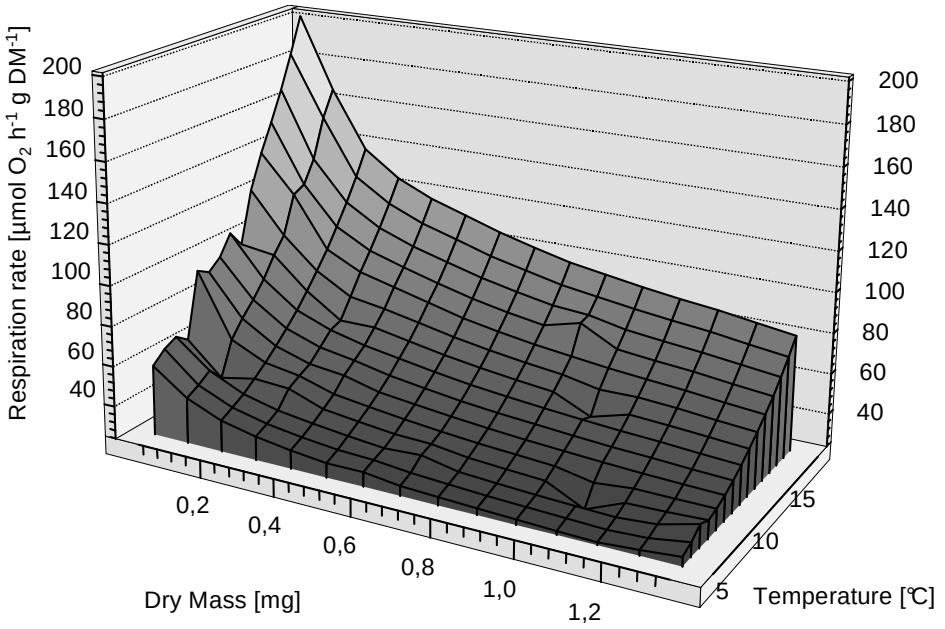

a)

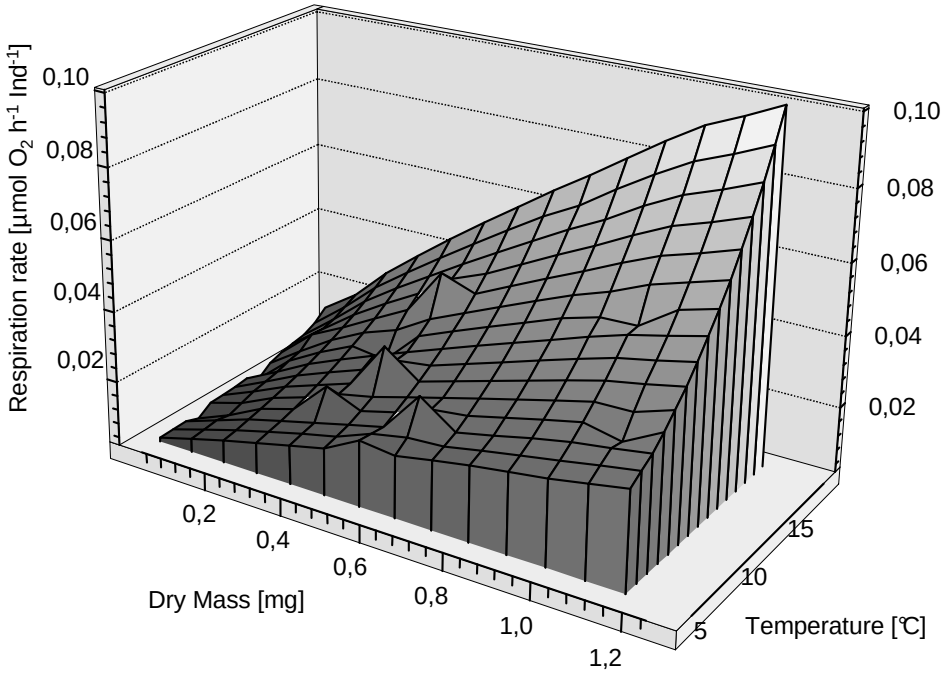

b)

Figure 20: a) The mass-specific and b) the individual respiration rates plotted against dry mass and temperature. Mean measured values at habitat temperatures were added to the model to see their deviation from calculated values. They can be identified as the peaks and valleys in the model.

3.3. Respiratory Electron Transport System Activity of Copepods

3.3.1. Electron Transport System Activity at Habitat Temperatures

Activity of the electron transport system (ETS) was measured in nine copepod species (Table 6). The activities ranged from 13.9 to 126 µmol O_2 h^{-1} g WM^{-1} and 0.006 to 0.199 µmol O_2 h^{-1} Ind^{-1}.

Between 6°C and 8°C, the highest mass-specific ETS-activities were measured in *Pleuromamma robusta* (31.6 ± 4 µmol O_2 h^{-1} g WM^{-1}). The lowest activities were detected in diapausing copepodids C5 of *Calanoides carinatus* (13.9 ± 2.8 µmol O_2 h^{-1} g WM^{-1}) and females of *Eucalanus hyalinus* (14.3 ± 1.4 µmol O_2 h^{-1} g WM^{-1}). Considering individual ETS-activities, *E. hyalinus* (0.128 ± 0.022 µmol O_2 h^{-1} Ind^{-1}) exhibited the highest activity, whereas diapausing C5s of *C. carinatus* (0.006 ± 0.002 µmol O_2 h^{-1} Ind^{-1}) also had the lowest individual ETS-activity.

Between 13°C and 16°C, the highest mass-specific ETS-activities were measured in copepods as *Aetideus armatus* (125 ± 8 µmol O_2 h^{-1} g WM^{-1}) and *N. minor* (94.5 ± 4 µmol O_2 h^{-1} g WM^{-1}), whereas the *E. hyalinus* (28 ± 4 µmol O_2 h^{-1} g WM^{-1}) and females of *Rhincalanus nasutus* (43 ± 10 µmol O_2 h^{-1} g WM^{-1}) had the lowest mass-specific ETS-activities. In contrast, *E. hyalinu*s (0.199 ± 0.053 µmol O_2 h^{-1} Ind^{-1}) and females of *R. nasutus* (0.085 ± 0.016 µmol O_2 h^{-1} Ind^{-1}) showed the highest individual ETS-activities, while the smallest copepod *Metridia lucens* (0.025 ± 0.002 µmol O_2 h^{-1} Ind^{-1}) and copepodite stages C4 of *R. nasutus* (0.032 ± 0.007 µmol O_2 h^{-1} Ind^{-1}) had the lowest.

Table 6: Wet mass-specific and individual ETS-activities of nine copepod species at respective habitat temperatures. Mean values are stated with standard deviation (± SD) while n denotes the number of replicates. Of *R. nasutus* and *C. carinatus* two different stages were measured. For the origin of the species see Table 4.

Species	Stage	T [°C]	Wet mass [mg]	ETS-activity		
				[µmol O_2 h^{-1} g WM^{-1}]	[µmol O_2 h^{-1} Ind^{-1}]	n
Aetideus armatus	f	15	0.420 ± 0.032	125.2 ± 8.2	0.052 ± 0.004	6
Nannocalanus minor	f	15	0.528 ± 0.044	94.5 ± 4.4	0.050 ± 0.004	6
Calanoides carinatus	f	13	0.541 ± 0.075	86.8 ± 4.1	0.047 ± 0.001	5
Metridia lucens	f	14	0.366 ± 0.034	68.0 ± 1.6	0.025 ± 0.002	3
Rhincalanus nasutus	C4	13	0.648 ± 0.191	50.7 ± 6.4	0.032 ± 0.007	6
Rhincalanus nasutus	f	13	2.032± 0.450	43.3 ± 10.2	0.085 ± 0.016	9
Pleuromamma robusta	f	8	2.714± 0.730	31.6 ± 4.1	0.087 ± 0.029	6
Eucalanus hyalinus	f	16	7.240 ±2.240	28.3 ± 4.2	0.199 ± 0.053	6
Pleuromamma xiphias	f	7	4.143 ± 0.540	21.0 ± 4.8	0.086 ± 0.018	5
Pleuromamma quadrungulata	f	6	3.824 ± 0.580	20.9 ± 2.4	0.079 ± 0.011	6
Eucalanus hyalinus	f	8	8.965 ± 1.48	14.3 ± 1.4	0.128 ± 0.022	6
Calanoides carinatus	C5	8	0.454 ± 0.031	13.9 ± 2.8	0.006 ± 0.002	6

3.3.2. Effect of Body Mass on ETS-activity

The mass-specific electron transport system (ETS) activities declined while individual ETS-activities increased with increasing body mass of the copepods (Figure 21, 22). To exclude the temperature effect the ETS measurements were grouped into a) 6 – 8°C and b) 13 – 16°C. The declines of the regression lines in Figure 21 and the increases of the lines in Figure 22 were significantly different from zero (p-values < 0.0001). In both plots the slopes were not significantly different from each other (p-values = 0.2). However, the differences of the Y-intercepts were significant due to generally higher ETS-activities at higher temperatures (p-values < 0.0001).

For mass-specific ETS-activities the following allometric equations were derived:

$$\text{Group a: } Y(\mu mol\ O_2 h^{-1} g\ WM^{-1}) = 46.77\ W^{-0.55}$$

$$\text{Group b: } Y(\mu mol\ O_2 h^{-1} g\ WM^{-1}) = 60.3\ W^{-0.44}$$

For individual ETS-activities the allometric equations were:

$$\text{Group a: } Y(\mu mol\ O_2 h^{-1} Ind^{-1}) = 0.047\ W^{0.45}$$

$$\text{Group b: } Y(\mu mol\ O_2 h^{-1} Ind^{-1}) = 0.06\ W^{0.56}$$

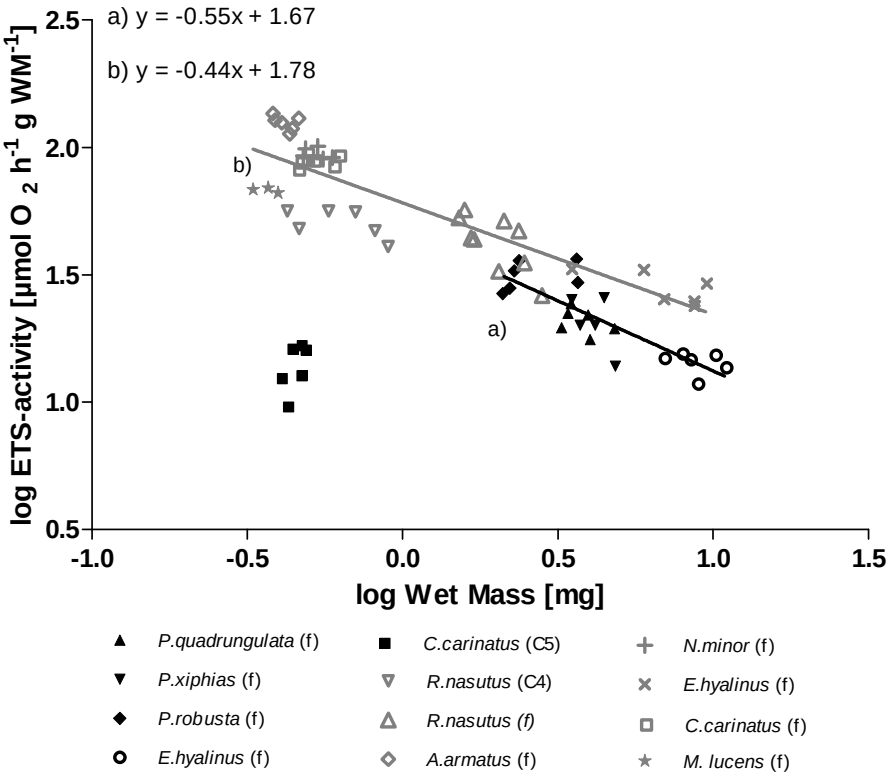

Figure 21: Relationship between log mass-specific ETS-activity and log wet mass (all specimens of all species) categorized in a) 6-8°C (black) and b) 13-16°C (grey). The extremely low ETS-activities of diapausing C5s of *C. carinatus* were not taken into account for the calculation. Equations of the linear regression analysis are shown. For a) $r^2 = 0.69$, p-value < 0.0001 and b) $r^2 = 0.75$, p-value < 0.0001. To differentiate the species, each species was given a symbol explained in the legend beneath the graph.

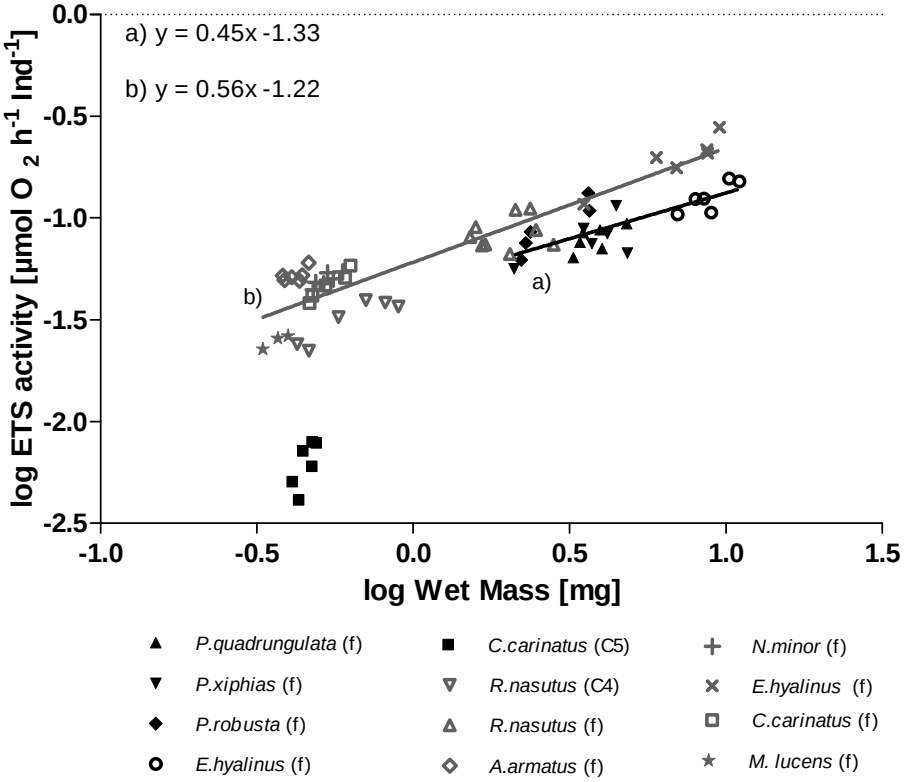

Figure 22: Relationship between log individual ETS-activity and log wet mass (all specimens of all species) categorized in a) 6-8°C (black symbols) and b) 13-16°C (grey symbols). The extremely low ETS-activities of C5s of *C. carinatus* were not taken into account for the calculation. Equations of linear regression analysis are shown. For a) $r^2 = 0.6$, p-value < 0.0001 and b) $r^2 = 0.82$, p-value < 0.0001. To differentiate the species, each species was given a symbol explained in the legend beneath the graph.

Dependence of ETS-activity on Body Mass and Temperature

To see whether there is a similar effect of body mass and temperature on ETS-activities than on the *in vivo* respiration, another model was constructed. It was derived from all measured ETS-activities, wet masses and habitat temperatures (Figure 23) except diapausing copepodids C5 of *Calanoides carinatus* were again excluded.

90.4% of the variance of the mass-specific ETS-activities was explainable by differences in wet mass (X_1) and habitat temperature (X_2) ($r = 0.951$, $r^2 = 0.904$), whereas 85.8% of the variance of the individual ETS-activities could be explained ($r = 0.926$, $r^2 = 0.858$). The

influence of both wet mass and temperature on the ETS-activity was statistically significant (p-values < 0.0001). The following equations were derived:

$$\log(Y\ \mu mol\ O_2 h^{-1} g\ WM^{-1}) = \log(26.9) - 0.459 \times \log(X_1) + 0.025 \times X_2$$

$$\log(Y\ \mu mol\ O_2 h^{-1} Ind^{-1}) = \log(0.027) + 0.541 \times \log(X_1) + 0.025 \times X_2$$

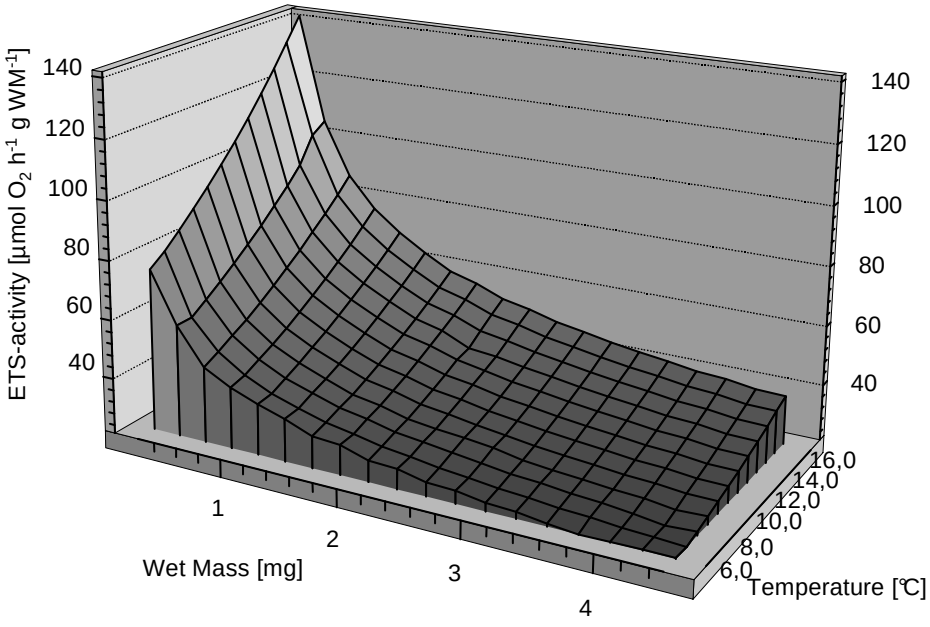

a)

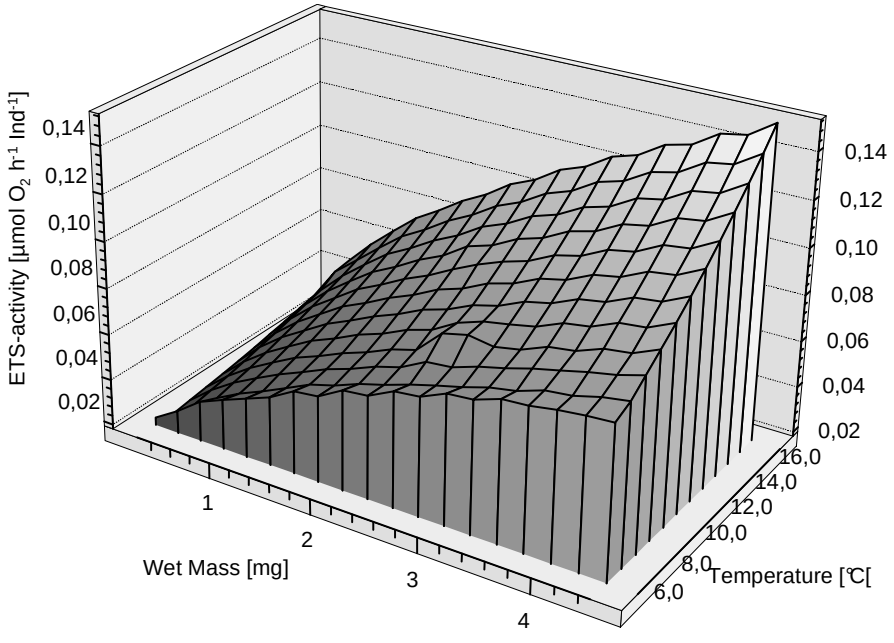

b)

Figure 23: a) The mass-specific and b) individual ETS-activities plotted against wet mass and habitat temperature. Mean measured values were added to the model to see their deviation from calculated values.

3.3.3. Relationship Between ETS-activity and Respiration Rate

The ETS-activity showed a significantly positive correlation with the measured respiration rates (Figure 24, p-value < 0.0001). Their relationship may be expressed as ETS:R or R:ETS ratios (Table 7) and are used for predictive purposes: The ETS:R illustrates the magnitude of which the ETS-activities exceeds the respiration rates, whereas the R:ETS gives the factor by which the measured ETS-activity of each species has to be multiplied to receive the respiration rate. The R:ETS ratios varied between 0.1 and 0.6. Copepodite stages C4 and females of *Rhincalanus nasutus* and deeper-living *Eucalanus hyalinus* had the lowest R:ETS ratios between 0.1 and 0.16. The highest ratio of 0.6 was calculated for diapausing copepodids C5 of C*alanoides carinatus*. No correlation between the ratios and temperature (p-value = 0.45) or body mass (p-value = 0.799) was detected.

Table 7: The ETS:R and R:ETS ratios were calculated from mean individual respiration rates and ETS-activities in nine copepod species at respective *in situ* temperatures. Of *R. nasutus* and *C. carinatus*, two different stages were measured. The letter for each species identifies its location in Figure 24.

Species	Stage	T [°C]	ETS-activity [µmol O_2 h^{-1} Ind^{-1}]	Respiration rate [µmol O_2 h^{-1} Ind^{-1}]	ETS:R	R:ETS
Eucalanus hyalinus (a)	f	16	0.199 ± 0.053	0.061 ± 0.021	3.2	0.309
Eucalanus hyalinus (b)	f	8	0.128 ± 0.022	0.019 ± 0.015	6.7	0.149
*Pleuromamma robusta (*c)	f	8	0.087 ± 0.029	0.031 ± 0.015	2.9	0.343
Pleuromamma xiphias (d)	f	7	0.086 ± 0.018	0.031 ± 0.015	2.8	0.360
Rhincalanus nasutus (e)	f	13	0.085 ± 0.016	0.013 ± 0.01	6.4	0.156
Pleuromamma quadrungulata (f)	f	5-6	0.079 ± 0.011	0.025 ± 0.001	3.2	0.315
Aetideus armatus (g)	f	15	0.052 ± 0.004	0.013 ± 0.001	4.0	0.251
Nannocalanus minor (h)	f	15	0.050 ± 0.004	0.012 ± 0.004	4.3	0.233
Calanoides carinatus (i)	f	13	0.047 ± 0.001	0.015 ± 0.0062	3.2	0.308
Rhincalanus nasutus (j)	C4	13	0.032 ± 0.007	0.003 ± 0.002	9.6	0.104
Metridia lucens (k)	f	13 - 14	0.025 ± 0.002	0.008 ± 0.001	3.3	0.306
Calanoides carinatus (l)	C5	8	0.006 ± 0.002	0.005 ± 0.001	1.7	0.600

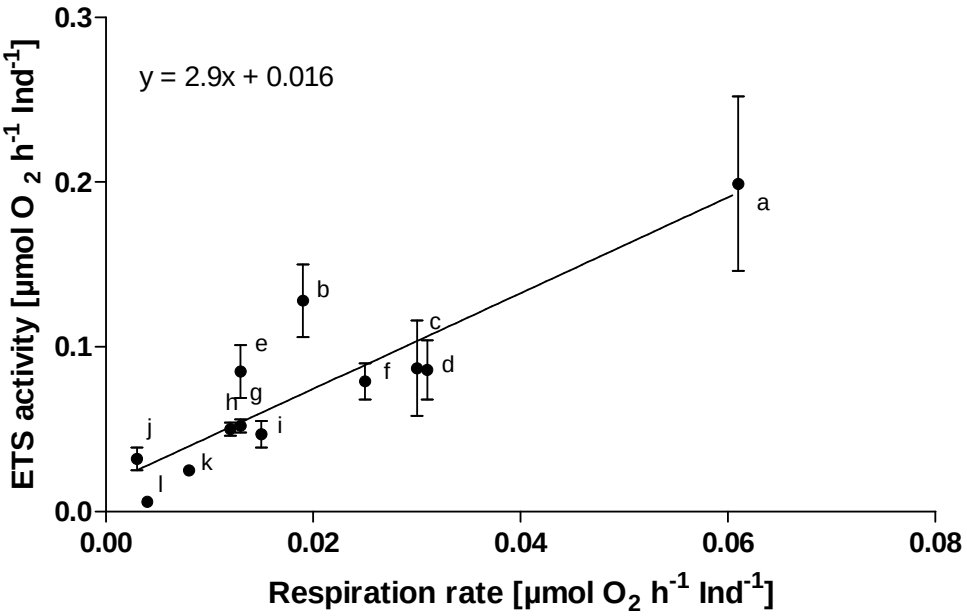

Figure 24: The dependence of ETS-activity on respiration rate is shown by linear regression analysis (r^2 = 0.8, p-value < 0.0001). Mean ETS-activities are shown with standard deviations (see Table 8).

3.4. Lactate Dehydrogenase Activity of Copepod Species

At pH 7.2 LDH-activity was detected in three species, whereas at pH 5.8 LDH-activity was measured in all eight species (Table 8). The activities ranged from 2.3 to 39.5 U g WM^{-1}. However, the subtraction of a reaction blind was resigned since they showed too high variability from negative to positive slopes (Figure 25a). To correct for unspecific reaction, the reaction was started as soon as the initial value was stable. A reaction was measured if all triplicate measurements showed similar decreases (Figure 25b).

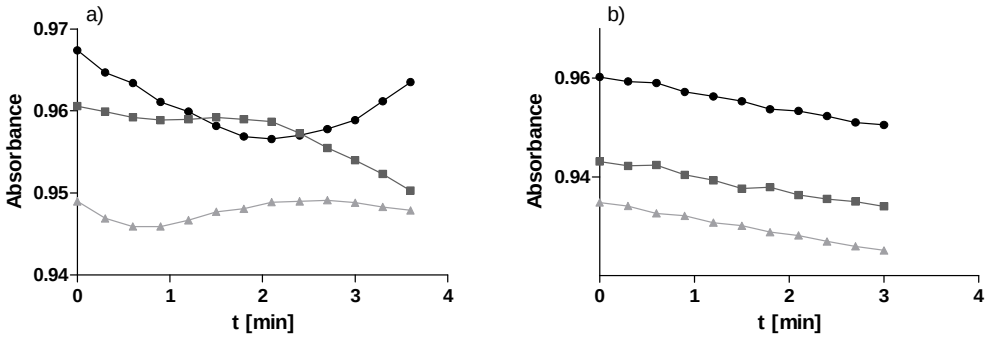

Figure 25: Absorbance in a triplicate measurement of a) a reaction blank and b) an example of *Atideus armatus*.

The highest LDH-activity of 39.5 ± 5 U g WM^{-1} was measured in *Rhincalanus nasutus* at pH 5.8, whereas the activity at pH 7.2 was significantly lower with 15 ± 3 U g WM^{-1} (p-value = 0.0008). In contrast, *Eucalanus hyalinus* had the second highest LDH-activity of 24 ± 4 U g WM^{-1} at pH 7.2 and significantly lower activities at pH 5.8 with 8 ± 1 U g WM^{-1}(p-value < 0.0001). *Pleuromamma xiphias* exhibited LDH activities of 6.5 ± 2 U g WM^{-1} at pH 7.2 and 5 ± 1 U g WM^{-1} at pH 5.8 (p-value = 0.4). No reactions could be measured at pH 7.2 in *Pleuromamma robusta*, *Nannocalanus minor*, *Calanoides carinatus* (C5, f), *Metridia lucens* and *Aetideus armatus*. However, at pH 5.8 *P. robusta* and *A. armatus* showed LDH-activities of 5.3 ± 1 U g WM^{-1} and 4.9 ± 1.5 U g WM^{-1}, respectively, while activities measured in *N. minor*, *C. carinatus* (C5, f) and *M. lucens* were between 2.3 and 3.4 U g WM^{-1}. The LDH-activities of *E. hyalinus* (p-value = 0.001) and *R. nasutus* (p-value = 0.011) were significantly higher compared to all other species. Mass-specific LDH-activities increased significantly with increasing body mass (p-value < 0.0001) while the scaling coefficient was 0.68 (Figure 26).

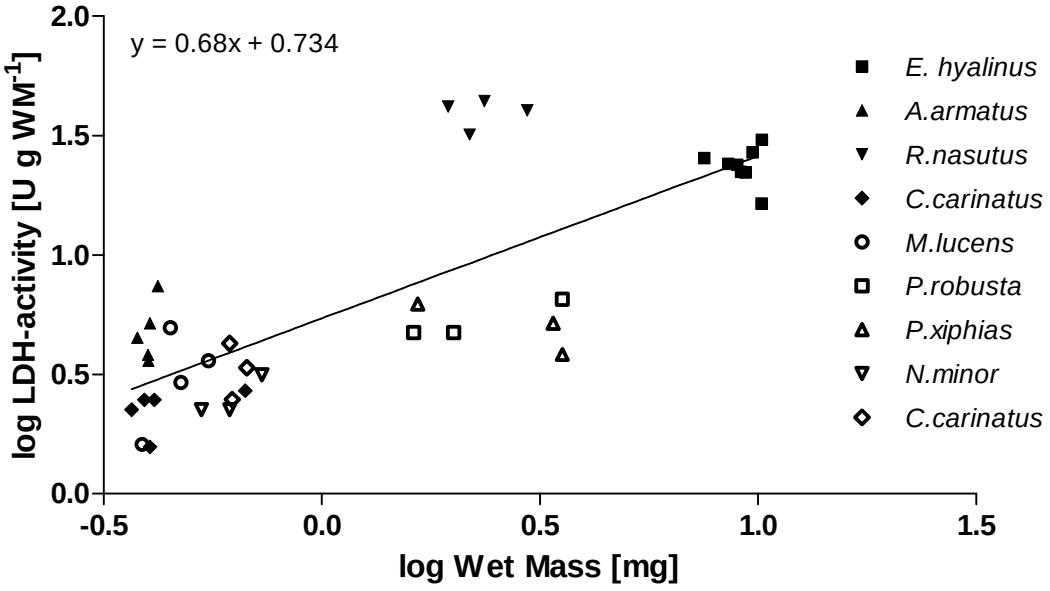

Figure 26: Log transformed LDH-activity is plotted against log body mass. To differentiate the species, each species was given a symbol explained in the legend next to the graph (r^2 = 0.61, p-value < 0.0001).

Table 8: The LDH-activities are given for eight copepod species in U g WM^{-1} (± SD) measured at pH 5.8 and 7.2. Stations and sampling depths with the respective oxygen range are stated. The number of replicates is given in parentheses.

Species	Stage	Station	Sampling depth [m]	Oxygen range [ml L^{-1}]	Wet mass [mg]	LDH-activity [U g WM^{-1}]	
						pH 5.8	pH 7.2
Rhincalanus nasutus	f	236	1000-800	3.5 - 4	2.520 ± 0.40	39.5 ± 5.31 (3)	14.8 ± 2.99 (3)
Eucalanus hyalinus	f	240	100 – 50	3.9 – 4.6	9.214 ± 0.90	8.25 ± 1.28 (8)	23.95 ± 4.05 (3)
Pleuromamma xiphias	f	238	600 – 400	1.5 – 3.2	2.871 ± 1.05	5.08 ± 1.21 (3)	6.53 ± 2.28 (3)
Pleuromamma robusta	f	236	600-400	1.9 - 3	2.604 ± 1.06	5.33 ± 1.04 (3)	2.36 ± 1.17 (4) (no reaction)
Nannocalanus minor	f	250	100 – 50	3.3 – 4.7	0.625 ± 0.10	2.55 ± 0.52 (3)	0.90 ± 0.23 (3) (no reaction)
Calanoides carinatus	C5	236	600 – 400	1.9 – 3	0.449 ± 0.12	2.30 ± 0.43 (5)	1.31 ± 0.8 (5) (no reaction)
	f	233	50 – 25	2 – 3	0.638 ± 0.03	3.37 ± 0.90 (3)	1.20 ± 0.47 (3) (no reaction)
Metridia lucens	f	225	100 – 60	2 – 3	0.466 ± 0.07	3.27 ± 1.39 (4)	1.43 ± 1.50 (3) (no reaction)
Aetideus armatus	f	254	100 – 50	1.6 – 3.8	0.401 ± 0.02	4.90 ± 1.50 (5)	0.46 ± 0.62 (4) (no reaction)

4. Discussion

4.1. Respiration of Copepods

Individual respiration rates varied from 0.04 to 1.57 µL O_2 h^{-1} Ind^{-1} which is in close agreement to the range of 0.05 to 4.17 µL O_2 h^{-1} Ind^{-1} that has been measured in subarctic copepods (Ikeda et al. 2006). The respiration rates measured in this study generally agreed with published data (Table 9, 10). For example, in deep-living copepodids C5 of *Calanoides carinatus* from the Benguela upwelling region a respiration rate of 0.12 µL O_2 h^{-1} Ind^{-1} was measured which coincides with the values derived in this study (0.14 ± 0.03 µL O_2 h^{-1} Ind^{-1}) (Arashkevich and Drits 1997). Significantly lower oxygen consumption rates were reported for copepodids C5 from surface and deep layers in the northern Benguela system (Kosobokova et al. 1988, Auel et al. 2005), whereas other C5s from surface layers showed higher respiration rates (Auel et al. 2005).

The respiration of copepods is dependent on intrinsic factors of the animal, e.g. its activity and maturity level, which may cause large inter- and intraspecific variations (Arashkevich and Drits 1997). In deep diapausing animals the respiration is reduced to a minimum. Deep-living copepodids C5 of *C. carinatus* from the Benguela Current system showed a reduction of respiration rates by 96% in comparison to surface-dwelling active individuals (Auel *et al.* 2005). In contrast, in other deep-living C5s a metabolic reduction of 25 – 30% compared to surface individuals was estimated (Kosobokova *et al*. 1988). The different respiration rates in copepodids C5 may be associated with their level of activity, as some animals may have been at the beginning or already at the end of their dormant stages. An increase in respiration was observed in moulted females due to increasing energetic losses during gonad maturation (Arashkevich and Drits 1997). In copepodids C5 of *C. Carinatus* and females of *Rhincalanus nasutus,* high lipid contents were correlated with reduced metabolic rates (Arashkevich et al. 1996, Ohman et al. 1998). The low metabolic rates and larger body mass of copepodids C5 in this study (125 ± 28 µg) compared to females of *C. carinatus* (99 ± 7 µg) was typical for diapause.

A large part of the deviations among the respiration rates measured in different studies may be explained by different geographical regions, temperatures and body masses. Often

body masses are not stated in other studies which make comparisons difficult. Methodological factors and differences in the experimental procedures, e.g. sampling methods, handling of copepods, time after capture, crowding, light, etc., further limit the comparability of different studies (Ikeda 1985, Pavlova 1994).

Table 9: Comparison of the individual respiration rates from this study with published data. Mean rates are given, if possible, ± standard deviation and dry mass in parentheses.

		This study		Published data		
Species	**Stage**	**T°C**	**Respiration rate [µL O_2 h^{-1} Ind^{-1}]**	**T°C**	**Respiration rate [µL O_2 h^{-1} Ind^{-1}]**	**Author**
Nannocalanus minor	f	15	0.26 ± 0.101 (97 µg)	26.9	0.21 ± 0.01 (40 µg)	Ikeda et al. 2001
Metridia lucens	f	13	0.17 ± 0.016	15.5	0.315	Raymont 1959
Calanoides carinatus	f	13	0.325 ± 0.139	16	0.472 ± 0.324	King and Packard 1975
				10	0.053 ± 0.01	Kosobokova et al. 1988
				11	0.31	Arashkevich and Drits 1997
				13-15	0.59 ±0.14	Arashkevich and Drits 1997
Calanoides carinatus	C5	8	0.142 ± 0.029	10	0.042 ±0.002*	Kosobokova et al. 1988
		13	2.258 ± 0.1	14	0.16 ± 0.1	Kosobokova et al. 1988
				8	0.12	Arashkevich and Drits 1997
Euchirella rostrata	f	10	0.325 ± 0.024 (480 µg)	3	0.558 (930 µg)	Ikeda et al. 2007
Pleuromamma xiphias	f	7	0.692 ±0.14	3	0.472 (563 µg)	Ikeda et al. 2007
			(644 µg)	12	0.549 (387 µg)	Ikeda et al. 2007
				28.4	1.14 (240 µg)	Gaudy and Boucher 1983
Geatanus pileatus		7	0.046 ± 0.006	5	0.035 – 0.038	Gaudy 1975

*Stage was not specified

Table 10: Comparison of the mass-specific respiration rates from this study with published data. Mean rates are given, if possible, ± standard deviation and dry mass in parentheses.

		This study		Published data		
Species	**Stage**	**T°C**	**Respiration rate [µL O_2 h^{-1} mg DM^{-1}]**	**T°C**	**Respiration rate [µL O_2 h^{-1} mg DM^{-1}]**	**Author**
Euchirella rostrata	f	10	0.688 ± 0.119 (480 µg)	3-5	0.83 (909 µg)	Conover and Corner 1968
Pleuromamma xiphias	f	7	1.08 ± 0.025 (644 µg)	28.5	4.82 (240 µg)	Gaudy and Boucher 1983
Pleuromamma robusta	f	8	1.58 ±0.664 (383 µg)	3-5	0.93 (362 µg)	Conover and Corner 1968
Rhincalanus nasutus	f	13	0.836 ± 0.547 (364 µg)	3-5	0.39 (529 µg)	Conover and Corner 1968
				10	0.033	Champalbert and Gaudy 1972
				14	0.143	Champalbert and Gaudy 1972
				18	1.59	Champalbert and Gaudy 1972
Calanoides carinatus	f	13	3.301 ± 1.323 (99 µg)	22	6.9 (120 µg)	Auel et al. 2005
		19	6.815 ± 2.27 (156 µg)			
Calanoides carinatus	C5	8	0.955 ± 0.268 (125 µg)	8	0.21 ± 0.08 (156 µg)	Auel et al. 2005
				20	5.23 (92 µg)	

4.2. Electron Transport System Activity of Copepods

The electron transport system (ETS) activity varied from 0.14 µL O_2 h^{-1} Ind^{-1} in copepodids C5 of *Calanoides carinatus* to 4.46 µL O_2 h^{-1} Ind^{-1} in females of *Eucalanus hyalinus*. This is within the range of 0.1 to 9.15 µL O_2 h^{-1} Ind^{-1} measured within 50 copepod species from the western subarctic Pacific (Ikeda et al. 2006).

Although several studies about zooplankton and ETS measurements have been published, knowledge of individual activities of copepods is rare (Table 11). Numerous studies measured community ETS-activities (Packard et al. 1971, Packard et al. 1975, Ahmed et al. 1976, Båmstedt 1980, Packard and Williams 1981, Schalk 1988, Naqvi and Shailaja 1993, Arístegui and Montero 1995). However, the ETS of *C. carinatus* has been studied quite well. The ETS-activities of copepodite stages C5 of *C. Carinatus* from 600 to 300 m depth (0.1 – 0.14 µL O_2 h^{-1} Ind^{-1}) are in agreement to the activities measured in this study (0.14 µL O_2 h^{-1} Ind^{-1}). Though, animals from 500 to 200 m (0.5 µL O_2 h^{-1} Ind^{-1}) and from the surface (0.61 – 1.32 µL O_2 h^{-1} Ind^{-1}) showed considerably higher ETS-activities most likely due to different activity levels (Arashkevich et al. 1996).

The ETS-activities in surface females of *C. carinatus* (0.88 and 1.21 µL O_2 h^{-1} Ind^{-1}) lie well within the standard deviation of the values measured in this study (1.05 µL O_2 h^{-1} Ind^{-1}) (Arashkevich et al. 1996). In contrast, activities in females of *C. Carinatus* measured by Kosobokova et al. (1988) and King and Packard (1975) were significantly lower than in females from this study. Not only different maturity levels (before or after spawning) but also methodological differences may account for these variations.

In general, the ETS-assay is quite sensitive. Errors in pipetting during measurements or preparation of the solutions may cause changes in the reaction and thus, may lead to different results. Four major factors could be identified strongly affecting the results. (1) The exact amount of zooplankton tissue for the assay is often not given. It was suggested that the homogenate should contain less than 5 mg wet mass per ml (Owen and King 1975). Our study shows significant differences depending on the dilution of copepod tissue to 1, 2, 3, 4 or 5 mg/ml. (2) In literature, a much higher concentration (1.5 mg/ml) of Polyvinylpyrrolidone (PVP) was used for the assay (Packard 1971, Packard et al. 1971, Owens and King 1975, Kenner and Ahmed 1975, Packard and Williams 1981). Due to the

severe decrease of ETS-activity, a lower PVP concentration was applied for the measurements. (3) Incubation times vary from 10 to 40 min (Packard 1971, Kenner and Ahmed 1975, Owens and King 1975, King and Packard 1975, Packard and Williams 1981, Schalk 1988, Simčič and Brancelj 1997). The tests in this study showed that the incubation time was species-specific and varied from 20 to 70 min. (4) The authors mentioned above used a quench solution after incubation and then measured the absorbance. No stopper solution was used in this study because the assays were measured sequentially with a 50 s offset. Quenched solutions may induce undesired side-reactions if the time interval between addition and measurement is too large (Koppelmann, personal communication).

Relationship of Respiration and Electron Transport System

The activity of the respiratory electron transport system (ETS) was positively correlated with the respiration rates of the different copepod species confirming the findings of King and Packard (1975) and Packard and Williams (1981).

The ratio of respiration to ETS-activity (R:ETS) reflects the fraction of the maximum respiratory capacity that an organism is effectively using (Simčič and Brancelj 1997). Surface *Rhincalanus nasutus* and deeper-living *Eucalanus hyalinus* exploited merely 10 – 16% of their potential metabolic rates, whereas the respiration rate of copepodids C5 of *Calanoides carinatus* was 60% of their ETS-activity. The ETS-activity of C5s of *C. carinatus* was extremely reduced indicating that the animals were in diapause. In contrast, all other species exploited between 20 and 36 % of their potential metabolic rate. R:ETS ratios are independent of temperature (King and Packard 1975, Lampert 1984) which was confirmed in this study. Thus, the lower R:ETS of the deeper-living *E. hyalinus* may reveal a much lower energy demand likely due to generally lower activities which have been shown in deeper-living animals (Schalk 1988).

The R:ETS ratios have been observed to be highly variable in different phyla while respiration seemed to be the factor causing such high variability. The R:ETS varied with the seasons and were positively correlated to primary production, thus, food availability and feeding activities (Hernandes-Léon and Gómez 1996). In zooplankton communities the R:ETS was described to be 0.38 while 0.5 was reported for *Calanus pacificus* (Owens

and King 1975, Bigidaire et al. 1982). For other crustaceans as e.g. *Acetes* (Decapoda) R:ETS ranged from 0.16 to 0.3 (Ikeda and Skjoldal 1980). The ratios for copepod species in this study varied from 0.1 to 0.6.

The R:ETS derived from previous studies are compared with own results in Table 11. Although the ETS-activities were generally lower, the range of R:ETS ratios from 0.56 to 1.08 for copepodids C5 and 0.27 for females of *C. carinatus* from the Benguela Current measured by Kosobokova et al. (1988) applied well to 0.6 and 0.31 calculated in this study. For different copepod species an R:ETS of even 1.45 to 2.79 was calculated (King and Packard 1975). Higher *in vivo* respiration rates than ETS-activities are quite unexpected. The ETS-assay measures the potential capacity of the metabolic rate. In contrast, the *in vivo* respiration measurements most likely depict the animals' routine metabolism, with uncontrolled but minimal motor activity (Ikeda 1985). Thus, ETS-activities were expected to exceed the respiration rates at least by 100%, which agrees with the results of this study (Packard et al. 1974). On average, individual ETS-activities were even four times higher than individual respiration rates in this study.

The earlier hypothesis, that ETS-activities are positively correlated with respiration rates, could be accepted. Measuring ETS-activities may provide a representative but relative indication of respiration rates. However, the high variability of the R:ETS ratios shows that there is no universal ratio to calculate copepods' respiration from ETS-activities. Ratios need to be established for each species from different depth layers to receive accurate respiration rates. Therefore, more data collection will be needed to validate the results of this study and to calculate ratios for a larger species range.

Table 11: Comparison of the ETS-activities from this study with published data. Sampling depths, R:ETS ratios and mean individual or mass-specific ETS-activities are given, if possible, ± standard deviation.

Species	Stage	This study				Published Data				Author
		Depth [m]	T°C	ETS-activity [µL O_2 h^{-1} Ind^{-1}]	R:ETS	Depth [m]	T°C	ETS-activity [µL O_2 h^{-1} Ind^{-1}]	R:ETS	
Clanoides carinatus	f	100-50	13	1.054 ± 0.178	0.31	50-0	10	0.88		Arashkevich et al.1996
						50-10	15	1.21		
						50-0	10	0.197± 0.02	0.269	Kosobokova et al. 1988
							16	0.255 ± 0.187*	1.98	King and Packard 1975
Calanoides carinatus	C5	600-400	8	0.142 ± 0.035	0.6	50-0	10	0.61	0.46	Arashkevich et al. 1996
						40-10	8	1.32		
						70-0	10	0.99		
						500-200	8	0.5		
						400-300	10	0.14		
						500-300	7	0.1		
						600-400	10	0.21		
						50-0	14	0.203 ± 0.02	0.79	Kosobokova et al. 1988
						500-200	10	0.046 ± 0.005	0.56	
							10	0.06 ± 0.01	1.08	
							10	0.075 ± 0.004	0.56	
Rhincalanus nasutus	f	50-25	13	1.906 ± 0.36	0.16			1.5 – 2		Ohman et al. 1998
				ETS-activity µL O_2 h^{-1} mg WM^{-1}				**ETS-activity µL O_2 h^{-1} mg WM^{-1}**		
Eucalanus hyalinus	f	50-25	16	0.633 ± 0.094	0.3		17	0.103		Flint et al. 1991
		400-300	8	0.320 ± 0.031	0.15					

4.3. Temperature Effect on Respiration Rates

Temperature had a significantly positive effect on respiration rates of the copepods. Usually an increase of 10°C would increase the respiration rate by the factor 2 to 4 for copepods (Mauchline 1998). The Q_{10} of *Metridia lucens*, *Calanoides carinatus* (C5) and *Pleuromamma quadrungulata* measured in this study were between 2 and 3.7, whereas *Eucalanus hyalinus*, *Rhincalanus nasutus* (C2/3,C4) and females of *C. carinatus* showed substantially higher Q_{10} values between 5.5 to 6.8. In arctic copepods, Q_{10} values between 2.05 and 4.5 were detected, i.a. *Metridia longa* showed a value of 2 between 0 and 10°C (Hirche 1987). For *Pleuromamma xiphias* and *Eucalanus elongatus* from the Mediterranean, Q_{10} values of 2.44 (0-22°C) and 4.08 (10-22°C) were calculated, respectively (Gaudy 1975).

The Q_{10} values for respiration rates have been shown to vary with the habitat temperature to which the animal is adapted (Rao and Bullock 1954), the speed of temperature change and the length of time spent at a certain temperature (Bullock 1955). In previous studies, animals were acclimatized for at least one or two days before being used for experiments (Raymont 1959, Ikeda 1970). Possible excess respiration rates were described for the first 24 h after capture of the copepods due to handling (Gauld and Raymont 1953). Respiration rates in copepod species decreased to a more or less constant level after three days (Ikeda 1970). In this study, the time on board was restricted to only ten days which is why acclimatization time had to be reduced to a minimum of 12 h. This may have lead to stress-induced higher Q_{10} values. Because of the short experimental periods, starvation seemed not to be a factor here. The respiration of planktonic copepods declined not until two or three days after starving (Raymont 1959).

Copepodite stages C5 of *C. carinatus* had a lower Q_{10} value than adult females. This result is in line with the metabolic reduction during diapause. Dormant individuals are expected to react to a lesser extent to changing environmental conditions than active ones. Temperature-dependent changes in the metabolism may be more or less severe, depending on the organism's activity level (Hochachka and Somero 1973). If *R. nasutus* and *E. hyalinus* have reduced metabolic rates *per se* due to their passive lifestyle (own observation), this would go along with their high temperature sensitivity.

Higher Q_{10} values usually indicate that an animal is restricted to constant temperatures within its natural habitat and not used to undergo severe temperature changes. It is not clear if *R. nasutus* and *E. hyalinus* undergo diel vertical migrations (DVM). On the one hand, slight DVMs were reported for *R. nasutus* (Koslow and Ota 1981, Sameoto 1984, Castro et al. 1993, Su 1996) while other studies did not detect migratory behaviour (Vervoort 1946, Roe 1972, Wishner and Allison 1986, Ohman et al. 1998, Padmavati et al. 1998, Farstey 2001). *E. hyalinus* showed a bimodal distribution in the Mediterranean during day and night while the majority did not undergo DVMs (Andersen et al. 2004). Slight DVMs were observed in *Eucalanus inermis* while other species of *Eucalanus* did not show DVMs in the Humboldt Current (Hildalgo et al. 2005, Escribano et al. 2009). The high temperature sensitivity detected in these two species further supports the assumption that they do not undergo DVMs.

The fact that *C. carinatus*, *E. hyalinus* and *R. nasutus*, species where DVM is not clear, showed the highest Q_{10} values commends the earlier hypothesis that migrating species seemed to have a higher temperature tolerance due to experiencing regular temperature changes during their DVMs. *P. quadrungulata*, known as an extensive migrator (Andersen et al. 2001, 2004, Loick et al. 2005, Auel and Verheye 2007), showed the lowest Q_{10} values, thus, a high tolerance to changing temperatures. This also agrees with results derived for *P. xiphias* by Champalbert and Gaudy (1972). However, to truly accept this hypothesis, more data would be necessary, preferably with a larger range of species and longer acclimatization times.

4.4. Ecological and Physiological Factors

Considering body mass and temperature, *Euchirella rostrata*, *Eucalanus hyalinus*, *Rhincalanus nasutus* (f, C2/3, C4) and *Metridia lucens* showed lower than average mass-specific respiration rates while the latter two also had reduced mass-specific electron transport system (ETS) activities.

Although none of the species were caught in the intermediate oxygen minimum layer (IOML), due to the extremely low biomass within this zone, IOMLs were present during the

cruise and the animals may have migrated through them. The potential of some species to inhabit IOMLs may be reflected in their physiology and biochemical composition.

Similar to *E. hyalinus* and *R. nasutus*, *E. rostrata* appeared to be a non- or weak- migrant in the Mediterranean (Andersen et al. 2001). In the Arabian Sea, *E. rostrata* was found within the lower IOML where oxygen concentrations fell below 1 ml L^{-1} (Madhupratap and Haridas 1990), whereas *M. lucens* has been observed to migrate through IOMLs (Timonin 1997, Fabian et al, 2005, Loick et al. 2005). *Eucalanus spp.* was found to permanently inhabit IOMLs in the Arabian Sea and the Humboldt Current (Flint et al. 1991, Fabian et al. 2005, Escribano et al. 2009, Escribano et al. 2009, Hildalgo et al. 2010). Furthermore, *R. nasutus* is a well known species inhabiting IOMLs in different regions (Castro et al. 1993, Someoto 1986, Fabian et al. 2005, Auel and Verheye 2007, Schnack-Schiel 2008). They have been found in the tropical Pacific at oxygen concentrations below 0.13 ml O_2 L^{-1}, in the Arabian Sea at concentrations below 0.15 ml O_2 L^{-1} and in the Red Sea between 0.49 and 1.3 ml O_2 L^{-1} (Madhuprata et al. 2001, Schnack-Schiel et al. 2008). They may survive periods of starvation by retreating into the IOML and reducing their metabolic rate (Weikert 1980). Also in the Benguela Current *R. nasutus* was found within the IOML (Auel and Verheye 2007). A reduction of their metabolic rates may enable them to live in such low oxygen conditions.

In addition, the “lethargic” lifestyle (Flint et al. 1991) observed in *E. hyalinus* and *R. nasutus* coincides with their reduced respiration rates which may protect them from tactile and visual predators considering their transparent body (Castellani et al. 2005). Reduced metabolic rates were also detected in females of *Eucalanus califiornicus* and *R. nasutus* indicating a quasi dormancy in winter (Ohman et al. 1998). They seemed to be “event-driven” species that respond to environmental circumstances rather than to seasonal phenomena (Ohman et al. 1998). The ETS-activity was only reduced in copepodite stages C4 of *R. nasutus* indicating that the females of *E. hyalinus* and *R. nasutus* did exploit merely a very small fraction of their potential metabolic rate.

Considering its body mass, the carnivorous species *Geatanus pileatus* and *Candacia cheirura* had higher mean mass-specific respiration rates than expected. Carnivorous species are expected to have higher oxygen requirements. Their lifestyle is more active than the one of herbivorous or omnivorous species because they have to actively search

for and catch their prey (Raymont 1959, Mauchline 1998). However, the differences in respiration were not significant to similar sized copepods as the omnivorous *E. hyalinus* (p-value = 0.23) and herbivorous *C. carinatus* (p-value = 0.23), respectively (Mauchline 1998).

A decline of metabolic rates with increasing depth of occurrence has been found in several pelagic organisms suggesting lower respiration rates as a characteristic for deeper-living species (Packard et al. 1975, Childress 1971, 1975, Torres et al. 1982, Schalk 1988). In contrast, other studies did not detect any depth-related changes in metabolic rates (Devol 1981, Bigidaire et al 1981, Thuesen et al. 1998). Although copepods from deeper layers respired less than the ones from layers above 100 m in this study, the decrease of respiration seemed to be attributed to the lower temperatures. Reasonable Q_{10} values for each species would be necessary to reveal possible influences of pressure that might be disguised by temperature. Standardized to 16°C by means of its Q_{10}, the respiration rates of *E. hyalinus* from 400 – 300 m depth did not differ significantly to *E. hyalinus* from the surface layers (p-value = 0.7). In contrast, deep living *E. hyalinus* had much lower energy demands than surface ones based on their ratio of respiration to ETS-activity (see 4.2). *P. robusta* from 400 – 200 m depth had a significantly higher respiration rate than *P. robusta* from 600 – 400 m while having the same habitat temperature. This difference could be attributed to the fact that the former ones were smaller and were measured during the night while the latter were measured during daytime. The species of *Pleuromamma* undergo extensive nocturnal diel vertical migrations (Pavlova 1994, Mauchline 1998, Andersen et al. 2001, Andersen et al. 2004, Wilson and Steinberg 2010). In migrating *P. xiphias* the natural activity rhythm was maintained during respiration measurements and accounted for enhanced respiration at night (Pavlova 1994).

The remaining variance of the metabolic rates, which could not be explained by differences in body mass and temperature, was explainable to a large part by differences in ecological and physiological factors of the copepods. Environmental conditions such as oxygen concentrations and vertical distribution as well as physiological and behavioural patterns like diel vertical migration, level of maturity and the general activity of the animals seemed to play the most important role.

4.5. Lactate Dehydrogenase Activity of Copepods

The mean lactate dehydrogenase (LDH) activity measured in different copepod species varied between 2.3 and 39.5 U g WM^{-1} which is in close agreement to the range of 0.08 to 70 U g WM^{-1} that has been measured in deep-sea copepods (Thuesen et al. 1998). For instance, the activities of *Pleuromamma abdonminalis*, *Metridia princeps* and *Calanus pacificus* were 0.887 ± 0.241 U g WM^{-1}, 3.886 ± 0.666 U g WM^{-1} and 2.059 U g WM^{-1}, respectively. Moreover, LDH-activities of 0.7 to 0.8 U g WM^{-1} were detected at pH 7.2 in the non-migrating *Calanus pacificus* while higher activities of 1.5 to 2.5 U g WM^{-1} were measured at pH 5.8 (Gonzales and Quiñones 2002). In contrast, generally higher LDH-activities between 120 and 140 U g WM^{-1} were measured in the euphausiid *E. mucronata*, a species undergoing diel vertical migrations (DVM) through the intermediate oxygen minimum layer (IOML) (Gonzales and Quiñones 2002). Although the values in this study may be generally overestimated by approximately 2 U g WM^{-1} due to assumed insufficient correction, they fall well in the measured range of Thuesen et al. (1998) and Gonzales and Quiñones (2002) for copepods.

The higher LDH-activity of *E. hyalinus* at pH 7.2 may result from a higher physiological pH of the animals so that the LDH requires a higher pH for operating correctly. Poor buffer capacities in handling pH decreases may also account for the copepods in this study that exhibited higher LDH-activities at lower pH, exceptions were *E. hyalinus* and *P. xiphias* (Gonzales and Quiñones 2002).

Unlike the enzymes associated with aerobic metabolic rates, the mass-specific LDH-activity seemed to increase exponentially with body mass (Somero and Childress 1980). A similar positive correlation between LDH-activity and body mass was detected in meso- and bathypelagic fish which was interpreted as an adaptation to burst swimming as the drag increases with body size and relative swimming velocity (Somero and Childress 1980, Childress and Somero 1990). These authors suggest that larger animals need higher LDH-activities to maintain identical burst-swimming abilities. Furthermore, the LDH-activities of copepods from the California Current showed a significant increase in mass-specific LDH-activities as a function of body mass (Thuesen et al. 1998).

Due to low correlation coefficients, other factors than body mass were suggested to add to the different LDH-activities (Thuesen et al. 1998). Species that use burst swimming for searching food or mates may have higher LDH-activities than slowly cruising species. Furthermore, species migrating through the water column or staying within IOMLs may also need LDH-activities as metabolic support. Quiescent species are expected to have lower LDH-activities due to their reduced metabolic rates (Thuesen et al. 1998).

Low to almost no LDH-activities were detected in copepodids C5 of *C. carinatus* beneath the IOML as well as *N. minor* and females of *C. carinatus* above the IOML (Loick et al. 2005). *Pleuromamma spp.* may migrate through while *Eucalanus spp.* potentially inhabits IOMLs (Ohman et al. 1998, Madhupratap et al. 2001, Fabian et al. 2005, Escribano et al. 2009, Auel and Verheye 2007, Hildalgo et al. 2010). However, the higher activities of *P. xiphias*, *P. robusta* and *E. hyalinus* were rather an effect of their larger body mass. A*etideus armatus* had higher LDH activities than expected. This species conducts DVM and was observed to be an active swimmer in the laboratory. It was found in the eastern tropical Pacific among the dominant species within a pronounced IOML with oxygen concentrations permanently below 0.5 ml O_2 L^{-1} (Saltzman and Wishner 1997). Moreover, *R. nasutus* may live for longer periods in IOMLs (Castro et al. 1993, Sameoto 1986, loick et al. 2005, Auel and Verheye 2007, Schnack-Schiel 2008, see 4.5). The significantly raised LDH-activities indicate that metabolic reduction seemed to be not their only adaptation. Due to their passive lifestyle with low swimming activity, the high LDH-activity may not be attributed to burst swimming in *R. nasutus*.

Supporting the earlier hypothesis, higher activities of LDH may occur in species inhabiting IOMLs which may enable them to survive in such low oxygen waters. However, high LDH-activities seem not to be a prerequisite for species occurring in IOMLs. More measurements of species of similar sizes are necessary to identify other factors that influence LDH-activity.

4.6. Modelling Metabolic Rates with Body Mass and Temperature

The majority of the variance within the metabolic rates of the copepods could be explained by differences in body mass and temperature. The calculated values fit quite well to the measured *in situ* respiration rates and ETS-activities.

The correlation between respiration rates and body mass is expressed as $Y = a\,W^b$. By multiple regression analysis, a model was developed to predict respiration rates at a given body mass and habitat temperature. Both body mass and temperature had a significant effect on metabolic rates with body mass showing the greater influence. The model could explain 66.6% of the variance of the individual respiration rates and 50.8% of the mass-specific respiration rates. For mass-specific respiration rates the scaling coefficient b was – 0.272 and for individual respiration rates 0.729. In contrast, 90.4% and 85.8% of the variation of the ETS-activities could be explained by body mass and habitat temperature whereas the mass-specific scaling coefficient b was – 0.459 and 0.541 for individual ETS-activities. The scaling coefficients are in close agreement with published data.

Estimated scaling coefficients for mass-specific respiration rates vary between – 0.1 and – 0.4 while most values are close to – 0.25 (Fenchel 1974, Blueweiss et al. 1978, Platt and Silvert 1981, Moloney and Field 1989). Other studies calculated – 0.33 (Baldock et al. 1980, Banse and Mosher 1980, Platt and Silvert 1981, Heusner 1982). For zooplankton, a scaling coefficient of – 0.312 was calculated (Moloney and Field 1989) while– 0.214 was derived for marine copepods (Thuesen et al. 1998).

Scaling coefficients for individual respiration rates vary from 0.65 to 0.9 for endotherms, ektotherms and unicellular organisms (Hemmingsen 1960), from 0.7 to 0.9 for aquatic organisms (Hernàndez-Léon and Williams 2005) and from 0.6 and 0.79 for marine crustaceans (Ivelva 1980). Lower coefficients from 0.3 to 0.7 were reported for copepods from the eastern Atlantic (Champalbert and Gaudy 1972) while 0.8 and 0.9 was reported for boreal and subtropical copepod species (Vidal and Withledge 1982). For zooplankton species, significantly different scaling coefficients were derived varying from 0.83 for boreal, 0.691 for temperate to 0.54 for tropical species (Ikeda 1970). These differences of the coefficients were rather a consequence of combining animals from different phyla than of temperature (Vidal and Whitledge 1982).

Applying similar multiple regression analyses on respiration rates of epipelagic zooplankton, a scaling coefficient of 0.789 was derived for zooplankton and 0.8 for marine copepods (Ikeda 1985, Ikeda et al. 2001). In contrast to our model, 93 – 96% of the variance of oxygen consumption rates could be attributed to differences in body mass and habitat temperature (Ikeda et al. 2001). Ikeda used a much larger dataset with a temperature range of – 1.7 to 29°C accumulated over many years, whereas much less data points were used in this study which may lead to the worse fit of the model.

In contrast to respiration rates, ETS-activities show a slow response to rapid environmental changes which is advantageous because results are not biased by short-term factors as sampling and handling of the copepods (Båmstedt 1980, Lampert 1984, Schalk 1988). A new ETS-equilibrium is reached after three to four hours after the environmental changes (Båmstedt 1980). This may explain the lower variance of ETS-activities and the better fit of the model compared to the model applying respiration rates.

The mathematical model shows that predicting metabolic rates from parameters as body mass and temperature is possible and may simplify future measurements. However, collecting more metabolic data and including further independent variables such as oxygen or depths may increase its predictive accuracy. The model represents a first approach towards the goal of the GENUS (Geochemistry and Ecology of the Namibian Upwelling System) project to parameterize consumption and energy requirements of copepods which helps to understand nutrient and carbon fluxes within the Benguela Current ecosystem.

5. References

Ahmed SI, Kenner, R.A., King, F.D. (1976) Preservation of enzymic activity in marine plankton by low-temperature freezing. Mar. Chem. 4: 133-139

Andersen V, Gubanova A, Nival P, Ruellet T (2001) Zooplankton communitiy during the transition from spring bloom to oligotrophy in the open NW Mediterranean and effects of wind event. 2. Vertical distribution and migrations. J. Plankt. Res. 23: 243-261

Arashkevich EG, Drits AV (1997) Ecological-physiological indices of *Calanoides carinatus* (Kroyer) from the Benguela upwelling region: biochemical composition, respiration, and gonad development of various life stages. Oceanology 37: 513–519

Arashkevich EG, Drits AV, Timonin AG (1996) Diapause in the life cycle of *Calanoides carinatus* (Kroyer), (Copepoda, Calanoida). Hydrobiologia 320: 197–208

Aristegui J, Agusti S, Middleburg JJ, Duarte CM (2005) Zooplankton respiration. In: Del Geiorgio PA, Williams PJ (eds) Respiration in aquatic ecosystems. Oxford University Press, pp 181–205

Arístegui J, Montero MF (1995) The relationship between community respiration and ETS activity in the ocean. J. Plankt. Res. 17: 1563–1571

Auel H, Verheye HM (2007) Hypoxia tolerance in the copepod *Calanoides carinatus* and the effect of an intermediate oxygen minimum layer on copepod vertical distribution in the northern Benguela Current upwelling system and the Angola-Benguela Front. J. Exp. Mar. Biol. Ecol. 352: 234-243

Auel H, Hagen W, Verheye HM (2005) Metabolic adaptations and reduced respiration of the copepod *Calanoides carinatus* during diapause at depth in the Angola-Benguela Front and northern Benguela upwelling regions. Afr. J. Mar. Sci. 27: 653–657

Baldock BM, Baker JH, Sleigh MA (1980) Laboratory growth rates of six species of freshwater Gymnamoebia. Oecologia 47: 156-159

Båmstedt U (1980) ETS-activity as an estimator of respiratory rate of zooplankton populations. The significance of variations in environmental factors. J. exp. Biol. Ecol. 42: 267–283

Banse K, Mosher S (1980) Adult body mass and annuals production/biomass relationships of field populations. Ecol. Monogr. 50: 355–379

Bigidaire RR, King FD, Biggs DC (1982) Glutamate dehydrogenase and respiratory electron transport system activities in the Gulf of Mexico zooplankton. J. Plankt. Res. 4: 895-912

Binet D, Suisse de Sainte Claire E (1975) Le copépod planctonique *Calanoides carinatus*. Répartition et cycle biologique au large de la Côthe dIvoire. Cah. ORSTOM Sér. Ocßeanogr. 13: 15–30

Boyer DC, Hampton I (2001) An overview of the living resources of Namibia. . S. Afr. J. mar. Sci. 23: 5–35

Bullock TH (1955) Compensation for temperature in the metabolism and activity of poikilotherms. Biol. Rev. 30: 311–342

Castellani C, Robinson, C., Smith, T., Lampitt, R.S. (2005) Temperature affects respiration rates in *Oithona similis*. Mar. Ecol. Prog. Ser. 285: 129-135

Castro LR, Bernal PA, Troncoso VA (1993) Coastal intrusion of copepods: mechanisms and consequences on the population biology of *Rhincalanus nasutus*. J. Plankt. Res. 15: 501–515

Chance B (1955) Enzyme mechanisms in living cells. In: McElroy WD, Glass B (eds) A symposium of the meachnism of enzyme action, pp 819 pp.

Chance B, Williams GR, Holmes WF, Higgins J (1955) Respiratory enzymes in oxidative phosphorylation: III. The steady state. J. Biol. Chem. 217: 439–451

Childress JJ (1971) Respiratory rates and depth of occurence of midwater animals. Limnol. Oceanogr. 16: 104-106

Childress JJ (1975) The respiratory rates of midwater crustaceans as a function of depth of occurence and relation to oxygen minimum layer off Southern California. Comp. Biochem. Physiol. 50A: 787-799

Childress JJ (1977) Effects of pressure, temperature and oxygen on the oxygen consumption rate of the midwater copepod *Gaussia princeps*. Mar. Biol. 39: 19–24

Childress JJ, Seibel BA (1998) Life at stable low oxygen levels: adaptations of animals to oceanic oxygen minimum layers. J. Exp. Biol. 201: 1223–1232

Childress JJ, Somero GN (1990) Metabolic scaling: A new perspective based on scaling of glycolytic enzyme activities. Am. Zool. 30: 161-173

Conover RJ (1959) Regional and seasonal variation in the respiratory rate of marine copepods. Limnol. Oceanogr. 4: 259–268

Conover RJ (1960) The feeding behavior and respiration of some planktonic Crustacea. Biol. Bull. 119: 399–415

Devol AH (1981) Vertical distribution of zooplankton respiration in relation to the intense oxygen minimum zones in two British Columbia fjords. J. Plankt. Res. 3: 593-602

Duncombe Rae CM (2005) A demonstration of the hydrographic partition of the Benguela upwelling ecosystem at 26°40'S. Afr. J. Mar. Sci. 27: 617–628

Ekau W, Auel H, Pörtner HO, Gilbert D (2010) Impacts of hypoxia on the structure and processes in pelagic communities (zooplankton, macro-invertebrates and fish). Biogeosciences 7: 1669–1699

Ekau W, Verheye HM (2005) Influence of oceanic fronts and low oxygen on the distribution of ichthyoplankton in the Benguela and southern Angola Currents. Afr. J. Mar. Sci. 27: 629-639

Escribano R, Hidalgo P, Krautz C (2009) Zooplankton associated with the oxygen minimum zone system in the northern upwelling region of Chile during March 2000. Deep-Sea Res. Part II 56: 1083-1094

Farstey V (2001) Feeding and vertical distribution of the calanoid copepods *Rhincalanus nasutus* Giesbrecht and *Pleuromamma indica* Wolfenden in the seasonally mixed water column in the northern part of the Gulf of Aqaba. PhD Thesis, Jerusalem, Israel

Fenchel T (1974) Intrinsic rate of natural increase: The relationship with body size. Oecologia 14: 317–326

Gaudy R (1975) Etude de la respiration chez des copépods pélagiques méditerranéens (bassin occidental et Mer Ionienne) et de ses variations en fonction de la bathymétrie des espèces de leur origine géogrphique. Mar. Biol. 29: 109–119

Gaudy R, Boucher J (1983) Relationship between respiration, excretion (ammonia and inorganic phosphorus) and activity of amylase and trypsin in different species of pelagic copepods from an Indian Ocean equatorial area. Mar. Biol. 75: 37–45

Gauld DT, Raymont JEG (1953) The respiration of some planktonic copepods. II. The effect of temperature. J. Mar. Biol. Ass. U.K. 31: 447–460

Gonzales RR, Quiňones RA (2002) Short communication Ldh activity in Euphausia mucronata and Calanus chilensis: implications for vertical migration behaviour. J. Plankt. Res. 24: 1349–1356

Goss LB, Bunting DL (1980) Temperature effects in zooplankton respiration. Comp. Biochem. Physiol. 66A: 651-658

Harris RP, Wiebe PH, Lenz J, Skjoldal HR, Huntley M (2000) ICES zooplankton methodoloy manual. Academic Press, London

Heinrich AK (1969) On the tropical plankton communities in the western Pacific. J. Cons. Int. Explor. Mer. 33: 45–52

Helly J, Levin L (2004) Global distribution of naturally occurring marine hypoxia on continental margins. Deep-Sea Res. Part I 51: 1159–1168

Hemmingsen AM (1960) Energy metabolism as related to body size and respiratory surfaces, and its evolution. Rep. Steno Mem. Hosp. Nord. Insulinlab 9: 1–110

Hernández-Léon S, Gómez M (1996) Factors affecting the respiration/ETS ratio in marine zooplankton. J. Plankt. Res. 18: 239-255

Hernández-Léon S, Ikeda T (2005) Zooplankton respiration. In: Del Giorgio PA, Williams, P.J. le B. (ed) Respiration in aquatic ecosystems. Oxford University Press, pp 57-82

Heusner AA (1982) Energy metabolism and body size. 2. Dimensional analysis and energetic non-similarity. Respir. Physiol. 48: 13–25

Heymans JJ, Shannon LJ, Jarre A (2004) Changes in the northern Benguela ecosystem over three decades: 1970s, 1980s, 1990s. Ecol. Model. 172: 175–195

Hildalgo P, Escribano R, Morales CE (2005) Ontogenetic vertical distribution and diel migration of the copepod *Eucalanus inermis* in the oxygen minimum zone off northern Chile. J. Plankt. Res. 27: 519-529

Hirche H-J (1987) Temperature and plankton.II. Effect on respiration and swimming activity in copepods from Greenland Sea. Mar. Biol. 94: 347–356

Hochachka PW, Somero GN (1973) Strategies of biochemical adaptation. W.B. Saunders Company, Washington

Hochachka PW, Somero GN (1984) Biochemical Adaptation. Princeton University Press

Hochachka PW, Somero GN (2002) Biochemical Adaptation: Mechanism and Progress in Physiological Evolution. Oxford University Press, New York

Hopkins TL (1969) Zooplankton standing crop in the Arctic basin. Limnol. Oceanogr. 14: 80-85

Hopkins TL (1971) Zooplankton standing crop in the Pacific sector of the Antarctic. In: Biology of the Antarctic seas. IV. Llano GA, Wallen IE (Eds). Antarc. Res. Ser. 17: 347–362

Hutchings L, Verheye HM, Hugget JA, Demarcq H, Cloete R, Barlow RG, Louw D, de Silva A (2006) Variability of plankton with reference to fish variability in the Benguela current large marine ecosystem—An overview. Large Marine Ecosystems. 14

Ikeda T (1970) Relationship between respiration rate and body size in marine plankton animals as a function of the temperature of the habitat. Bulletin of the Faculty of Fisheries Hokkaido University 21: 91–112

Ikeda T (1974) Nutritional ecology of marine zooplankton. Memoirs of the Faculty of Fisheries Hokkaido University 22: 1–97

Ikeda T (1985) Metabolic rates of epipelagic marine zooplankton as a function of body mass and temperature. Mar. Biol. 85: 1–11

Ikeda T, Kanno Y, Ozaki K, Shinada A (2001) Metabolic rates of epipelagic marine copepods as a function of body mass and temperature. Mar.Biol. 139: 587–596

Ikeda T, Motoda S (1978) Zooplankton production in the Berring Sea calculated from 1956 - 1970 Oshoru Maru data. Mar. Sci. Comm. 4: 329–346

Ikeda T, Sano F, Yamaguchi A (2000) Oxygen consumption - Winkler titration. . In: Harris RP, Wiebe PH, Lenz J, Skjoldal HR, Huntley M (eds) ICES zooplankton methodology manual. Academic Press, San Diego, pp 493-499

Ikeda T, Sano F, Yamaguchi A (2007) Respiration in marine pelagic copepods: a global-bathymetric model. Mar. Ecol. Prog. Ser. 339: 215–219

Ikeda T, Sano F, Yamaguchi A, Matsuishi T (2006) Metabolism of mesopelagic and bathypelagic copepods in the wetsren North Pacific Ocean. Mar. Ecol. Prog. Ser 322: 199-211

Ikeda T, Skjoldal HR (1980) The effect of laboratory conditions on the extrapolation of experimental measurements to the ecology of marine zooplankton. 6. Changes in physiological activities and biochemical components of *Acetes sibogae australis* and *Acetes australis* after capture. Mar. Biol. 58: 285-294

Ivelva IV (1980) The dependence of crustacean respiration rate on body mass and habitat temperature. Int. Revue ges. Hydrobiol. 65: 1–45

Jarre-Teichmann A, Shannon LJ, Moloney CL, Wickens PA (1998) Comparing trophic flows in the southern Benguela to those in other upwelling systems. S. Afr. J. mar. Sci. 19: 391–414

John and Huber (2005) Instruction manual OXY- 10 software version OXY10v3_33FB. Precision Sensing GmbH

Kenner RA, Ahmed SI (1975) Measurements of electron transport activities in marine phytoplankton. Mar. Biol. 33: 119–127

King FD, Packard TT (1975) Respiration and the activity of the respiratory electron transport system in marine zooplankton. Limnol.Oceanogr. 20: 849–854

Kleiber M (1967) Der Energiehaushalt von Mensch und Haustier. Paul Parey, Hamburg

Koslow AJ, Ota A (1981) The ecology of vertical migration in three common zooplankters in the La Jolla Bight, April - August 1967. Biol. Oceanogr. 1: 107–134

Kosobokova KN, Krylov PI (1988) Physiological and biochemical characteristics of *Calanoides carinatus* in an upwewlling off the coast of Namibia. Oceanology 28: 375–379

Lampert W (1984) The measurement of respiration. In: Downing JA, Rigler, F.H. (ed) A manual on methods of the assessment of secondary productivity in fresh water. Black-well Scientific Publications, Oxford, pp 413-468

Lass HU, Schmidt M, Mohrholz V, Nausch G (2000) Hydrographic and current measurements in the area of the Angola-benguela Front. J. Phys. Ocenanogr. 30: 2598–2609

Loick N, Ekau W, Verheye HM (2005) Water body preferences of dominant calanoid copepod species in the Angola-Benguela frontal system. Afr. J. Mar. Sci. 27: 597–608

Longhurst AR (1985) The structure and evolution of plankton communities. Prog. Oceanogr. 15: 1–35

Longhurst AR, Harrison WG (1989) The biological pump: Profiles of plankton production and consumption in the upper ocean. Prog. Oceanogr. 22: 47–123

Madhupratap M, Gopalakrishnan TC, Haridas P, Nair KKC (2001) Mesozooplankton biomass, composition and distribution in the Arabian Sea during the Fall Intermonsoon: Implications of oxygen gradients. Deep-Sea Res. 48: 1345-1368

Madhupratap M, Haridas P (1990) Zooplankton, especially calanoid copepods, in the upper 1000 m of the south-east Arabian Sea. J. Plankt. Res. 12: 305-321

Mauchline J (1998) Advances in marine biology: The biology of calanoid copepods. Academic Press, London, UK

McMahon T (1973) Size and shape in biology. Science: 1201–1203

Mohrholz V, Heene T, Muller A, Hansen A (2011) GENUS TP2 cruise report - MSM17/3, on board

Moloney CL, Field JG (1989) General allometric equations for rates of nutrient uptake, ingestion, and respiration in planktonic organisms. Limnol. Oceanogr. 34: 1290–1299

Naqvi SWA, Shailaja MS (1993) Activity of the respiratory electron transport system and the respiration rates within the oxygen minimum layer of the Arabian Sea. Deep-Sea Res. 40: 687-695

Nelson G, Hutchings L (1983) The Benguela upwelling area. Prog. Oceanogr. 12: 333–356

Ohman MD, Drits AV, Clarke ME, al. (1998) Differential dormancy of co-occuring copepods. Deep-Sea res. Part II 45: 1709–1740

Owens TG, King FD (1975) The measurement of respiratory electron-transport-system activity in marine zooplankton. Mar. Biol. 30: 27–36

Packard TT (1971) The measurement of respiratory electron transport activity in marine phytoplankton. J. Mar. Res. 29: 235–244

Packard TT, Devol, A.H., King, F.D. (1975) The effect of temperature on the respiratory electron transport system in marine plankton. Deep-Sea Res. 22: 237-249

Packard TT, Harmon D, Boucher J (1974) Respiratory electron transport activity in plankton from upwelled waters. Tethys 6: 213–222

Packard TT, Healy ML, Richards FA (1971) Vertical distribution of the activity of the respiratory electron transport system in marine plankton. Limnol. Oceanogr. 16: 60-70

Packard TT, Williams PJleB (1981) Rates of respiratory oxygen consumption and electron transport in surface seawater from the northwest Atlantic. Oceanol. Acta 4: 351–358

Padmavati G, Haridas P, Nair KKC, Gobalakrishnan TC, Shiney P, Madhupratap M (1998) Vertical distribution of mesozooplankton in the central and eastern Arabian Sea during the winter monsoon. J. Plankt. Res. 20: 343-354

Pavlova EV (1994) Diel changes in copepod respiration rates. Hydrobiologia 292/293: 333–339

Peterson W (1998) Life cycle strategies of copepods in coastal upwelling zones. J. Mar. Syst. 15: 313–326

Pfaffenhöfer G-A (2006) Oxygen consumption in relation to motion of marine planktonic copepods. Mar. Eco. Prog. Ser. 317: 187–192

Platt T, Silvert W (1981) Ecology, physiology, allometry and dimensionality. J. Theor. Biol. 93: 855–860

Rao KP, Bullock TH (1954) Q10 as a function of size and habitat temperature in poikilotherms. Amer. Nat. 88: 33–44

Raymont JEG (1959) The Respiration of Some Planktonic Copepods. Limnol. Oceanogr. 4: 479–491

Raymont JEG (1983) Plankton and productivity in the oceans, Vol. 2. Pergamon Press, Oxford

Richardson AJ, Verheye HM, Herbert V, Rogers C, Arendse LM (2001) Egg production, somatic growth and productivity of copepods in the Benguela Current System and Angola-Benguela Front. S. Afri. J. Mar. Sci. 97: 251–257

Roe HSJ (1974) The vertical distributions and diurnal migrations of calanoid copepods collected on the SOND cruise, 1965. II. Systematic account: families Calanidae up to and including the Aetideidae. J. Mar. Biol. Assoc. UK 52: 315.343

Sameoto DD (1984) Environmental factors influencing diurnal distribution of zooplankton and ichthyoplankton. J. Plankt. Res. 6: 767–792

Schalk PH (1988) Respiratory electron transport system (ETS) activities in zooplankton and micronekton of the Indo-Pacific region. Mar. Ecol. Prog. Ser 44

Schiedek D (1997) *Marenzelleria viridis* (Verrill, 1873) (Polychaeta), a new benthic species within European coastal waters: Some metabolic features. J.Exp. Mar.Biol. Ecol. 211: 85–101

Schnack-Schiel SB, Niehoff B, Hagen W, Böttger-Schnack R, Cornils A, Dowidar MM, Pasternak A, Stambler N, Stübing D, Richter C (2008) Population dynamics and life strategies of *Rhincalanus nasutus* (Copepoda) at the onset of the spring bloom in the Gulf of Aqaba (Red Sea). J. Plankt. Res. 30: 655–672

Scholander PF, Flagg W, Walters V, Irving L (1953) Climate adaptation in arctic and tropical poikilotherms. Physiol. Zool. 26: 67–92

Shannon LV, Agenbag JJ, Buys MEL (1987) Large- and mesoscale features of the Angolar-Benguela front. S. Afr. J. Mar. Sci. 5: 11-34

Shannon LV, Nelson G (1996) The Benguela: large scale features and processes and system variability. . In: Wefer G, Berger WH, Siedler G, Webb DJ (eds) The South Atlantic: present and past circulation. Springer, Berlin pp 163–210

Shannon LV, O'Toole MJ (2003) Sustainability of the Benguela: ex Africa semper aliquid novi. In: Hempel G, Sherman K (eds) Large marine ecosystems: trends in exploitation, protection and research. Elsevier, Amsterdam

Shannon V (2006) A plan comes together. In: Shannon V, Hempel G, Malanotte-Rizzoli P, Moloney C, Woods J (eds) Benguela: Predicting a large marine ecosystem. Elsevier B.V., Amsterdam

Sherman K (2006) Forcasting within the context of large marine ecosystems progams. In: Shannon V, Hempel G, Malanotte-Rizzoli P, Moloney C, Woods J (eds) Benguela predicting a large marine ecosystem. Elsevier B.V., Amsterdam

Sičmič T, Brancelji A (1997) Electron transport system (ETS) activity and respiration rate in five Daphnia species at different temperatures. Hydrobiologia 360: 117–125

Somero GN, Childress JJ (1980) A violation of the metabolism-size scaling paradigm: Activities of glycolytic enzymes in muscle increase in larger-size fish. Physiol. Zool. 53: 322-337

Sommer U, Stibor H, Katechakis A, Sommer F, Hansen T (2002) Pelagic food web configurations at different levels of nutrient richness and their implications for the ratio fish production:primary production. Hydrobiologia 484: 11-20

Su CH (1996) Vertical migration of five dominant copepods in the northern South China Sea. MSc. Thesis, Keelung

Szela TL, Marsh AG (2005) Microtiter plate, optode respirometry, an inter-individual variance in metabolic rates among nauplii of *Artemia sp.* Mar. Ecol. Prog. Ser. 296: 281–289

Thuesen EV, Miller CB, Childress JJ (1998) Ecophysiological interpretation of oxygen consumption rates and enzymatic activities of deep-sea copepods. Mar. Ecol. Prog. Ser. 168: 95–107

Timonin AG (1997) Diel vertical migrations *of Calanoides carinatus* and *Metridia lucens* (Copepoda: Calanoida) in the northern Benguela upwelling area. Mar. Biol. 37: 782-787

Timonin AG, Arashkevich EG, Drits AV, Semenova TN (1992) Zooplankton dynamics in the northern Benguela ecosystem, with special reference to the copepod Calanoides carinatus. . S. Afr. J. Mar. Sci. 12: 545–560

Torres JJ, Belman BW, Childress JJ (1979) Oxygen consumption of midwater fishes as a function of depth of occurence. Deep-Sea Res. 26A: 185-197

Verheye HM (1991) Short-term variability during an anchor station study in the southern Benguela upwelling system. Abundance, distribution and estimated production of mesozooplankton with special reference to *Calanoides carinatus* (Krøyer, 1849). Prog. Oceanogr. 28: 91–119

Verheye HM, Hagen W, Auel H, Ekau W, Loick N, Rheenen I, Wencke P, Jones S (2005) Life strategies, energetics and growth characteristics of *Calanoides carinatus* (Copepoda) in the Angola-Benguela frontal region. Afr. J. Mar. Sci. 27: 641–651

Verheye HM, Hutching L, Peterson WT (1991) Life history and population maintenance strategies of *Calanoides carinatus* (Copepoda: Calanoida) in the southern Benguela ecosystem. S. Afr. J. Mar. Sci. 11: 179–191

Verheye HM, Hutchings L, Hugget JA, Painting SJ (1992) Mesozooplankton dynamics in the Benguela ecosystem, with emphasis on the herbivorous copepods. In: Benguela trophic functioning. Payne, A.I.L., Brink, K.H., Mann, K.H. and R. Hilborn (Eds). S. Afr. J. mar. Sci. 12: 561–584

Verity PG (1985) Ammonia excretion rates of oceanic copepods and implications for estimates of primary production in the Sargasso Sea. Biol. Oceanogr. 3: 249–283

Verwoor W (1993) Pelagic copepoda. part I. Copepoda Calanoida of the families Calanidae up to and including Euchaetidae. Atlantide-Rep. 7: 77–194

Weikert H (1980) The oxygen minimum layer in the Red Sea: Ecological implications of the zooplankton occurence in the area of the Atlantis II Deep. Meeresforsch. 28: 1-9

Wilson SE, Steinberg DK (2010) Autotrophic picoplankton in mesozooplankton guts: Evidence of aggregate feeding in the mesopelagic zone and export of small phytoplankton. Mar. Ecol. Prog. Ser 412: 11-27

Wishner KF, Allison SK (1986) The distribution and abundance of copepods in relation to the physical structure of the Gulf Stream. Deep-Sea Res. 33: 705–731

Internet Sources

http://de.academic.ru/pictures/dewiki/50/200px-NADNADH_svg.png

Acknowledgments

I would like to thank PD Dr. Holger Auel for accepting the supervision of my Master Thesis and for the opportunity I was given to take part in this project. I am very thankful for all his good advices and constructive comments.

Likewise, I would like to thank Dr. Werner Ekau for being my second supervisor of my Master Thesis.

I would like to thank Petra Wencke, Lena Teuber and Anna Schukat of the Marine Zoology Department who have been a great help and support and were always there to hear my questions and problems during the course of this study.

The crew and different GENUS teams for their help on board.

Rolf Koppelmann and Thorsten Werner for their constructive comments.

The Department of Marine Botany and Marine Microbiology for providing me with additional laboratory equipment.

Declaration

I herewith declare that I have completed the present thesis independently making use only of the specified literature and aids. Figures taken from other sources are identified as such.

Bremen, _____ _____

Maya Bode